Appl. Phys. B 60, 211–227 (1995)

Applied Physics B Lasers and Optics

Quantum dynamics of bouncing atoms in a stable gravitational cavity

G.J. Liston, S.M. Tan, D.F. Walls

Department of Physics, University of Auckland, Private Bag 92019, Auckland, New Zealand
(Fax: +64-9/373-7445, E-mail: GJL@phyvc.auckland.ac.nz)

Received: 4 August 1994 / Accepted: 9 November 1994

Abstract. Two-level atoms bouncing in a stable gravitational cavity are considered, where the atomic mirror at the bottom of the bounces is an evanescent wave caused by an internally reflected intense Gaussian-mode laser beam. We consider the broadening mechanisms of the atoms from their initially tightly spaced position distribution, using a phenomenological semi-classical model, which includes spontaneous emission. A fully quantum model, which neglects spontaneous emission, is derived, and the broadening of the atomic wave function in the quantum model is compared with the broadening of the atomic distribution in an analogous classical simulation where spontaneous emission is similarly neglected. We find that the broadening is correctly described by the classical simulations in the horizontal directions, while it significantly underestimates the broadening in the vertical direction.

PACS: 32.80.Pj

Progress in atomic optics has been rapid since the first demonstrations of atomic interference several years ago [1–4]. One current goal of atomic optics is to achieve a Fabry-Perot-type interferometer for atomic de Broglie waves [5–7]. As a first step towards the Fabry-Perot interferometer, a gravitational cavity has been considered. This involves bouncing atoms vertically on a curved mirror formed from an evanescent wave. The curvature of the mirror ensures that the classical trajectories close to the vertical axis are stable. Several experimental groups have reported successful demonstrations of atoms in this "trampoline" configuration [8–10]. The most successful experiment has been that recently reported by Aminoff et al. [10]. In their experiment, a cold cloud of cesium atoms was dropped onto the mirror and up to ten successive bounces were observed.

In this paper, we present an analysis of atoms bouncing in such a gravitational cavity. We first present a semi-classical simulation where the momentum and position of the atom are well defined. The effects due to spontaneous emission when the atom interacts with the evanescent wave are included using a Monte-Carlo calculation. We calculate the spreading of the initial position distribution of the atoms due to the initial velocity distribution and the effects of spontaneous emission. In particular, we observe the effect of state changes between the two dressed energy eigenstates. This broadening mechanism was observed experimentally and analyzed theoretically by Seifert et al. [11], for argon atoms reflecting off an evanescent wave at a glancing incidence. We further give a fully quantum analysis of the atom bouncing in the gravitational cavity by direct calculation of the time-dependent Schrödinger equation. Spontaneous emission is neglected in the quantum calculations. The spreading of the atomic position distribution is calculated and is compared with analogous classical simulations where the spontaneous emissions are similarly neglected. We find that, while the classical simulations adequately describe the spreading in the x and y (horizontal) directions, it greatly underestimates the spreading in the z- (vertical) direction.

Dedicated to H. Walther on the occasion of his 60th birthday

1 Configuration

The configuration we consider consists of an intense Gaussian-mode laser beam totally internally reflected off a prism of glass, with a concave spherical region having been polished into its top surface. This creates an evanescent wave extending from the glass surface into the vacuum above it, and the electric field of this wave, if positively detuned with respect to the atomic-transition frequency, causes a quasi-potential which is used as the mirror for the bouncing atoms. Two-level atoms from a trap are dropped onto the evanescent wave, and bounce repeatedly inside the stable configuration (Fig. 1). Using a classical field, we can write the Hamiltonian as

$$H = H_A + V + H_G \,, \tag{1}$$

where

$$H_A = \frac{\mathbf{p}^2}{2m} + \hbar\omega_0 b^\dagger b \,, \tag{2}$$

$$H_G = mgz \,, \tag{3}$$

$$V = -\mathbf{d}\cdot\left[b^\dagger \mathbf{E}^*(\mathbf{R},t) + b\mathbf{E}(\mathbf{R},t)\right] \,, \tag{4}$$

and H_A is the Hamiltonian term referring to the energy of the atom, V refers to the interaction with the classical light

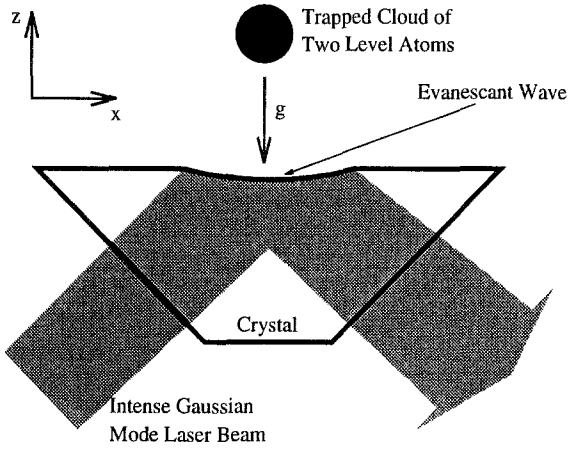

Fig. 1. Schematic diagram of the configuration for the stable gravitational cavity

field, and H_G is due to gravity. For the interaction term, **d** is the dipole moment of the atom, **E** is the electric field due to the laser, and **R** is the position operator. For the atomic term in the Hamiltonian, m is the mass of the atom, ω_0 is the atomic transition frequency, and $b = |g\rangle\langle e|$, where $|g\rangle$ and $|e\rangle$ refer to the ground and excited states of the two level atom. In H_G, g is the gravitational constant, and z is the position operator in the z-direction.

Converting to the interaction picture removes the simple evolution due to $H_0 = \hbar\omega_L b^\dagger b$, where $\omega_L = \omega_0 + \delta$, ω_L being the frequency of the laser, and δ the detuning from the atomic-transition frequency. Diagonalizing the Hamiltonian, while excluding the kinetic-energy term, we find two dressed states $|+\rangle$ and $|-\rangle$,

$$|+\rangle = \sin\Theta(\mathbf{R})|g\rangle + \cos\Theta(\mathbf{R})|e\rangle\,, \tag{5}$$

$$|-\rangle = \cos\Theta(\mathbf{R})|g\rangle - \sin\Theta(\mathbf{R})|e\rangle\,, \tag{6}$$

where

$$\mathbf{d}\cdot\mathbf{E}(\mathbf{R}) = \frac{\hbar}{2}\omega_1(\mathbf{R}) \tag{7}$$

and

$$\cos 2\Theta(\mathbf{R}) = \frac{-\delta}{\Omega(\mathbf{R})}\,, \quad \sin 2\Theta(\mathbf{R}) = \frac{\omega_1(\mathbf{R})}{\Omega(\mathbf{R})}\,, \tag{8}$$

$$\Omega(\mathbf{R}) = \sqrt{\delta^2 + \omega_1(\mathbf{R})^2}. \tag{9}$$

We find the energy eigenfunctions of the $|+\rangle$ and $|-\rangle$ states to be

$$\frac{E_\pm(\mathbf{R})}{\hbar} = -\frac{\delta}{2} \pm \frac{\Omega(\mathbf{R})}{2} + \frac{m}{\hbar}gz\,. \tag{10}$$

If we were using a plane crystal, then the electric field due to the evanescent wave would have the form

$$\mathbf{E}(\mathbf{R}) = \mathbf{E_0}\exp\left[-\alpha z - \left(\frac{x}{\omega_x}\right)^2 - \left(\frac{y}{\omega_y}\right)^2\right] e^{ik_x x}\,, \tag{11}$$

where ω_x, ω_y are the waist dimensions of the beam at the crystal in the xy-plane, α is the decay constant in the z-direction, $\mathbf{E_0}$ is the maximum electric field, and k_x is the wave number in the x-direction, where the xz-plane is the plane of incidence of the laser. Due to the fact that we are using a concave crystal, with radius of curvature R, z must be replaced by z', where

$$\begin{aligned} z' &= z - \left[R - \sqrt{R^2 - (x^2+y^2)}\right] \\ &\approx z - \frac{1}{2R}(x^2+y^2) \end{aligned} \tag{12}$$

for $(x^2+y^2) \ll R^2$, where the approximation is exact if we replace the spherical curvature with a quadratic curvature. Hence, we can write

$$\begin{aligned} \mathbf{E}(\mathbf{R}) = \mathbf{E_0}\exp\Bigg[-\alpha z + \left(\frac{\alpha}{2R} - \frac{1}{\omega_x^2}\right)x^2 \\ + \left(\frac{\alpha}{2R} - \frac{1}{\omega_y^2}\right)y^2\Bigg] e^{ik_x x} \end{aligned} \tag{13}$$

and we obtain ω_1 in the form

$$\begin{aligned} \omega_1(\mathbf{R}) = \omega_{1_{\max}}\exp\Bigg[-\alpha z + \left(\frac{\alpha}{2R} - \frac{1}{\omega_x^2}\right)x^2 \\ + \left(\frac{\alpha}{2R} - \frac{1}{\omega_y^2}\right)y^2\Bigg]\,. \end{aligned} \tag{14}$$

2 Semi-classical model

For our semi-classical simulation, we make several approximations. First, we assume that the momentum and position of the atom are both well defined at all times. Second, we assume that the atom is traveling slowly enough that the adiabatic approximation is valid, so that, if the atom enters the evanescent wave in a $|+\rangle$ state, it will stay in a $|+\rangle$ state, feeling a repulsive force due to the positively detuned light field. If a spontaneous emission occurs, we know the atom must be in the ground state, which we can write as a superposition of $|+\rangle$ and $|-\rangle$ states. Our last assumption is to neglect the coherences between these $|+\rangle$ and $|-\rangle$ states, by probabilistically choosing one of these states at each spontaneous emission, and resolving the atom to be in either the $|+\rangle$ or $|-\rangle$ state.

In the region where the evanescent wave is negligible, the evolution of the atom is exactly the same as for Galilean kinematics, and in the evanescent wave, the force on the atom is $\mathbf{F} = -\nabla(E_\pm)$, depending on whether the atom is in the $|+\rangle$ or $|-\rangle$ state. We determine whether a spontaneous emission has occurred by evolving the atom over a short time $\mathrm{d}t$, and then comparing the probability of a spontaneous emission in that time period with a random number between 0 and 1. If $P_e\Gamma\mathrm{d}t$ is greater than the chosen random number, where P_e is the probability the atom is in the excited state, and Γ is the rate of spontaneous emissions, then a spontaneous emission occurs. At the time when this happens, the atom gets a kick in momentum that can be determined from the momentum direction of the spontaneously emitted photon, which is chosen randomly, with weighting

$$\Pr(\text{emission into } \mathrm{d}\Omega) = \frac{3}{16\pi}\left(1+\cos^2\theta\right)\mathrm{d}\Omega \tag{15}$$

for a circularly polarized light field, where θ is the angle between the direction of the spontaneously emitted photon and the incident radiation, and

$$\Pr(\text{emission into } d\Omega) = 3/8\pi \sin^2 \rho \, d\Omega \qquad (16)$$

for a linearly polarized light field, where ρ is the angle between the polarization direction of the light field and the wave vector of the emitted light. These weightings have an overall negligible effect as compared to an unweighted distribution, where the photon is spontaneously emitted with equal probability in all directions.

We then resolve the atom to be in the $|+\rangle$ or $|-\rangle$ state, as mentioned above, and continue the evolution. The only way an atom can be lost is if in the course of its evolution it reaches a point which is below the surface of the crystal.

Our initial position distribution of ground-state atoms is chosen to be a spherically symmetric Gaussian, characterized by mean position r and standard deviation $\sigma(r)$. The velocity distribution is a Maxwell-Boltzmann distribution characterized by a temperature T. The Monte-Carlo type simulation proceeds by randomly choosing a position and a velocity according to the initial distributions, computing the evolution of the atom for a time period approximately equivalent to ten bounces, whilst recording the position of the atom at regular time steps. This procedure is repeated many times to obtain the overall effect.

We consider three effects that have a tendency to broaden the position distribution from its initial tightly spaced configuration. The first is simply the initial velocity distribution. If we neglect spontaneous emission, so that the atom starts and always remains in the $|+\rangle$ state, then two atoms incident upon the evanescent wave with the same position and velocity will always rebound in precisely the same manner. The only spreading is due to the initial variance in the velocity distribution, and the fact that atoms fall on different positions of the spherically shaped crystal. Secondly, the momentum kicks due to photons being spontaneously emitted results in a change of velocity of the atom and hence tends to spread the distribution. The dotted curve in Fig. 2 shows a possible resultant change in the position of an atom due to a single spontaneous emission, where the atom always remains in the $|+\rangle$ state. Lastly, the effects of a change in state of the atom can cause the position distribution for the atoms to be significantly broadened, and more of the atoms to be lost. If an atom undergoes a spontaneous emission, and is randomly chosen to undergo a state change to the $|-\rangle$ state, then it can be seen from (10) that the sign of the force the atom feels due to the interaction with the light field is reversed, and hence, instead of being repelled by the evanescent wave, it is attracted to regions of higher intensity. If no further spontaneous emissions occur, it will accelerate into the concave crystal and hence be lost from the simulation. If however, another spontaneous emission occurs, and the atom changes back to a $|+\rangle$ state, it may be re-ejected into the area above the evanescent wave, but significantly perturbed from its original path. If the potential changed while the atom was falling towards the crystal, it will be ejected from the evanescent wave with significantly more kinetic energy than it entered with, and if the potential changed while the atom was moving away from the crystal, then the atom would be significantly retarded or slowed down [11]. The solid curves in Fig. 2 plot a possible perturbation in the trajectory of an atom from its original path (dashed curve) for an atom undergoing a state change while both approaching (upper solid curve) and leaving (lower solid curve) the crystal. The oscillating curves in Fig. 3 show the number of atoms with z-positions between 2.3 and 3.3 mm above the crystal, for no spontaneous emission (dashed curve), spontaneous emission with no state changes (dotted curve), and with both spontaneous emission and state changes (solid curve). The plots underneath show the number of atoms lost in the respective simulations. The major broadening effect is clearly due to the influence of spontaneous emission, causing both an increased spread in the distribution of the particles, and an increased loss of particles. The added effect of the state changes is only slight, due mainly to the fact that the number of state change events is much less than the number of spontaneous emissions, especially if the atom has a small total energy compared to the detuning. Even if the atom does undergo a state change, the $|-\rangle$ state has the excited state as its major component, so the probability of another spontaneous emission becomes very large, and the atom rapidly returns to the $|+\rangle$ state. Hence, if the state change does occur, the overall effect is only slight as it feels the attractive force for such a short time, and the resultant change in velocity in the z-direction is small. Clearly the magnitude of all of these broadening mechanisms depends largely on the parameters chosen, and in particular on the total energy of the atom, the detuning and the spontaneous emission rate.

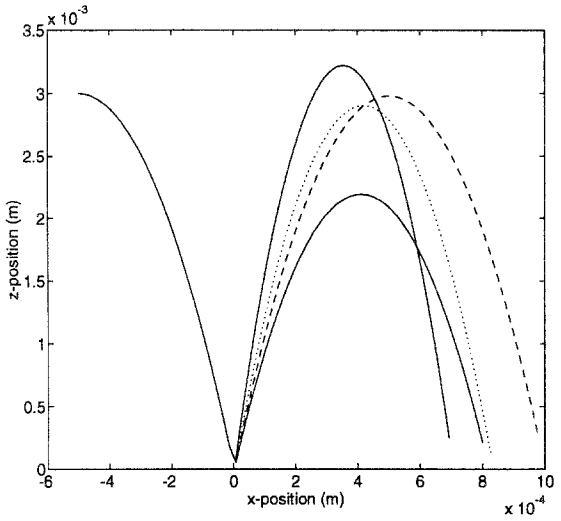

Fig. 2. Plot of some possible trajectories for an atom doing one bounce on the evanescent wave, where no spontaneous emissions occur (*dashed line*), one spontaneous emission occurs (*dotted line*) and a state change to a $|-\rangle$ state both approaching (*upper solid curve*) and leaving (*lower solid curve*) the crystal occurs

3 Quantum model

If we neglect spontaneous emission, so that the atom always remains in the $|+\rangle$ state, but do not use the classical approximation that the position and momentum of the atom are precisely defined, we must then consider the Time-dependent Schrödinger Equation (TDSE)

$$H\Psi(\mathbf{r}, t) = i\hbar \frac{\partial \Psi(\mathbf{r}, t)}{\partial t} , \qquad (17)$$

where the Hamiltonian H is defined by

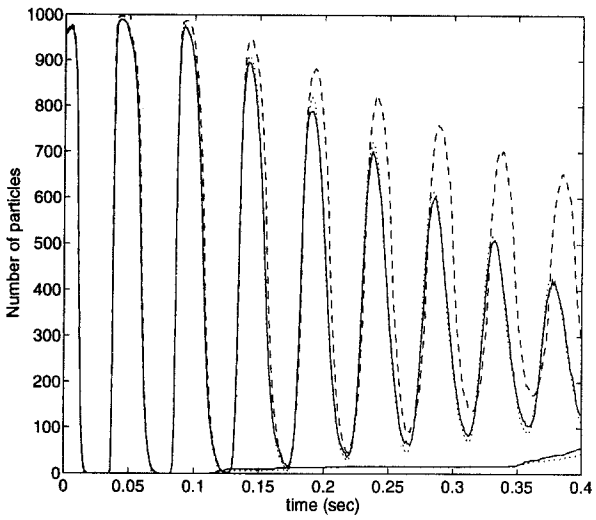

Fig. 3. The oscillatory plots show the number of atoms with z-positions between 2.3 and 3.3 mm, where there is no spontaneous emission (*dashed line*), spontaneous emission with no state changes (*dotted line*) and including state changes (*solid line*). The *bottom lines* show the total number of atoms lost. Note that no atoms are lost for the case when there is no spontaneous emission. Initial conditions were a spherically symmetric position distribution characterized by a mean position $r = 2.91$ mm, a standard deviation $\sigma(r) = 0.4$ mm, and a Maxwell-Boltzmann distribution in velocity characterized by a temperature $T = 0.5 \times 10^{-6}$K. Atomic parameters were those of cesium, having a spontaneous emission rate $\Gamma = 3.1 \times 10^7 \mathrm{s}^{-1}$, a mass $m/\hbar = 209.3 \times 10^7 \mathrm{kg/Js}$, with atomic transition frequency $\omega_0 = 852$ nm. The evanescent wave was characterized by a characteristic distance $1/\alpha$ where $\alpha = 4.76 \times 10^6\ \mathrm{m}^{-1}$, waists in the x- and y-directions $\omega_x = 1$ mm, $\omega_y = 1.1$ mm, a detuning $\delta = 1.9 \times 10^9\ \mathrm{s}^{-1}$, and $\omega_{1_{\max}} = 5.68 \times 10^9\ \mathrm{s}^{-1}$. The crystal has a radius of curvature $R = 2$ cm, and the gravitational constant $g = 9.8\ \mathrm{m/s}^2$

$$H = \frac{\mathbf{p}^2}{2m} + E_+(\mathbf{r})\,. \tag{18}$$

The most immediate problem is the choice of the coordinate system. Wallis et al. [6], considered an infinite potential rather than the actual rapidly exponentially decaying potential caused by the evanescent wave. The quantized energy eigenstates were calculated using a transformation to parabolic coordinates, which causes both the solution of the time-independent Schrödinger equation and the boundary conditions to be separable. If the exponentially decaying nature of the potential is included, then the boundary conditions are no longer separable and as such the transformation to parabolic coordinates is not useful. We note that if the Gaussian beam waists in the x- and y-directions (ω_x and ω_y) are different, then, even using the parabolic coordinate system, the loss of rotational symmetry around the vertical axis causes the boundary conditions to be inseparable. This problem, however, could be solved by a simple scaling of the x- and y-coordinates. A more fundamental problem with the use of the parabolic coordinate system for the stable gravitational cavity can be seen by considering the foci of the surfaces of constant potential, which a classical atom would be expected to just strike. Ignoring gravitational effects, and assuming the evanescent wave has the same waist in both horizontal directions, the surfaces of constant energy are paraboloids described by

$$z - f(E) = \left(\frac{1}{2R} - \frac{1}{\alpha\omega_x^2}\right)\left(x^2 + y^2\right)\,, \tag{19}$$

where

$$f(E) = \frac{1}{\alpha}\log\left(\frac{\omega_{1_{\max}}}{2\sqrt{\frac{E^2}{\hbar^2} + \frac{E\delta}{\hbar}}}\right) \tag{20}$$

In contrast to Wallis et al. [6], where the foci of the paraboloid reflecting surfaces at the bottom of the bounce remained in the same position for all energies, the foci of these paraboloids have z-value

$$z = f(E) + \frac{1}{\frac{2}{R} - \frac{4}{\alpha\omega_x^2}} \tag{21}$$

which depends non-trivially on the energy. Even in this classical situation then, the boundary conditions that apply for the motion of the atom cannot be separated using a transformation to parabolic coordinates, when the exponentially decaying nature of the potential is taken into account. We hence choose to retain a Cartesian coordinate system.

3.1 Methodology

In this paper, we wish to obtain the time-dependent behaviour of a wave packet which occupies a narrow range of energies and which remains reasonably well confined in space throughout the motion. The well-known technique for solving the TDSE for systems such as the one we are considering, is to solve the Time Independent Schrödinger Equation (TISE) to obtain the quantized energy eigenstates $\phi_n(\mathbf{r})$, and sum these together multiplied by a weighting c_n determined from the initial conditions, and a time-dependent phase factor

$$\Psi(\mathbf{r}, t) = \sum_n c_n \phi_n(\mathbf{r}) \mathrm{e}^{-\mathrm{i}E_n t/\hbar}\,. \tag{22}$$

Due to the nature of this problem, and in particular its intrinsic time dependence, we have chosen to use a different technique, which allows us to obtain a simple physical interpretation in terms of wave function parts traveling in different directions, and also avoids the need to calculate the modes. This subsection describes the method by considering a general one dimensional case, demonstrates its equivalence with the previously mentioned technique involving energy eigenstates, and discusses the added complications that occur when we extend to three dimensions.

We wish to solve the TDSE

$$-\frac{\hbar^2}{2m}\frac{\partial^2\Psi}{\partial x^2} + V(x)\Psi = \mathrm{i}\hbar\frac{\partial\Psi}{\partial t} \tag{23}$$

for a potential $V(x)$ which diverges to positive infinity as $x \to \pm\infty$, and so has a countable number of energy eigenstates. We shall suppose that the energies of interest correspond to high-order modes of the trap so that the wave function undergoes many oscillations between the classical turning points and the particle remains largely confined to the region between these classical turning points.

To introduce the notation used, we shall first describe the well-known "eigenstate" method of solving the TDSE.

Choosing two arbitrary points $-\infty < x_1 < x_2 < \infty$ divides the x-axis into three regions, and in the central region $x_1 < x < x_2$, solving the TISE gives two linearly independent solutions $u_E(x)$ and $u_E^*(x)$ for each energy which, without loss of generality, can be chosen to be complex conjugates. Any general solution in this range can be written as a linear combination of these two solutions

$$\Psi_E(x) = a_+(E)u_E^+(x) + a_-u_E^-(x) \,. \tag{24}$$

For the ranges $x < x_1$ and $x > x_2$, the solutions [$bw_E(x)$ and $cv_E(x)$, respectively] must satisfy the additional constraint that they cannot diverge as $x \to \pm\infty$, and so we are restricted to one linearly independent solution, which is chosen to be real. Matching the values and derivatives of the solutions at x_1 and x_2, we find the condition

$$\begin{pmatrix} A(E) & B(E) \\ C(E) & D(E) \end{pmatrix} \begin{pmatrix} a_+(E) \\ a_-(E) \end{pmatrix} = 0 \tag{25}$$

must be satisfied for an energy eigenstate, where A and B depend on the energy and are determined at the right-hand classical turning point

$$A = B^* = u_E(x_2)v_E'(x_2) - u_E'(x_2)v_E(x_2) \tag{26}$$

with C and D similarly determined at the left. For energies E_m, where condition (25) is fulfilled, that is, when the determinant of the coefficient matrix is zero, and so $a_+(E)$ and $a_-(E)$ have non-trivial solutions, we can define the energy eigenstate as

$$\phi_m(x) = \begin{cases} c_m w_m(x) \,, & x < x_1 \\ a_{+_m}u_m(x) + a_{-_m}u_m^*(x) \,, & x_1 < x < x_2 \\ b_m v_m(x) \,, & x > x_2 \,. \end{cases} \tag{27}$$

Using this set of eigenstates, we can write the general time-dependent solution at any time t as

$$\Psi(x,t) = \sum_m c_m\phi_m(x)\mathrm{e}^{-\mathrm{i}E_m t/\hbar} \,, \tag{28}$$

where $\Psi(x,0) = \sum_m c_m\phi_m(x)$ is the initial-position wave function.

To describe the technique used in the following subsections, we must first note that the solutions $u_E(x)$ and $u_E^*(x)$ can be chosen such that the phase of $u_E(x)$ is increasing in the positive x-direction, and that of $u_E^*(x)$ is increasing in the negative x-direction. This is particularly clear when the WKB approximation is valid, and we can write

$$\psi(x) = Ak(x)^{-\frac{1}{2}} \exp\left[\pm\frac{\mathrm{i}}{\hbar}\int^x k(x)\mathrm{d}x\right] \,, \tag{29}$$

where

$$k(x) = \{2m[E - V(x)]\}^{\frac{1}{2}} \tag{30}$$

We physically interpret $u_E(x)$ and $u_E^*(x)$ as wave functions traveling to the right or the left direction, as when multiplied by a time-dependent phase factor $\mathrm{e}^{-\mathrm{i}Et/\hbar}$, the constant phase moves to the right or the left for $u_E(x)$ and $u_E^*(x)$, respectively. Further, as we only require the time-dependent solution for positions between x_1 and x_2, we can allow $u_E(x)$ to take any form outside these points, as long as they can be linearly superposed inside this range to give an arbitrary general eigenstate (not constricted by the boundary conditions). In particular, it allows us to choose them to be delta-function normalizable, so the expansion of the initial condition is simple. Rather than solving for the modes of the entire system, the essence of the chosen technique lies in a consideration of the problem as two one-wall bouncing problems. Because only one boundary condition is considered at any point in the calculation, we retain a continuum of energies. Given the initial wave packet is predominantly moving in only one direction (say to the right), we expand our initial conditions in terms of the $u_E(x)$ only. Considering this as a one-wall reflection problem, we can determine the wave packet that will be reflected from the right-hand boundary. Similarly for this leftwards moving reflected wave packet, we consider it approaching the left wall as a one-wall reflection problem, and calculate the reflected wave packet, which is now traveling to the right. To solve the TDSE, we simply sum together all the infinite number of reflections from the sides.

We will now show that this is equivalent to the previous energy-eigenstate technique. If we consider an initial condition $\Psi(x,0)$ which is predominantly moving towards the right, then we can neglect the overlap with the states moving to the left $u_E^*(x)$, and we write

$$\Psi(x,0) = \int_0^\infty W(E)u_E(x)\mathrm{d}E \,. \tag{31}$$

For the wave function traveling in its initial course to the right, we write the time-dependent solution as

$$\Psi_1(x,t) = \int_0^\infty W(E)u_E(x)\mathrm{e}^{-\mathrm{i}Et/\hbar}\mathrm{d}E \,. \tag{32}$$

We can interpret the A and B terms above as reflection coefficients, so if we have a wave $u_E(x)$ "traveling" to the right, then the wave "traveling" to the left caused by the reflection of the first wave is simply $[a_-(E)/a_+(E)]u_E^*(x)$, where $a_+(E)$ and $a_-(E)$ are constricted by the boundary condition that their superposition must match a decaying wave as $x \to +\infty$. We know $A(E)a_+(E) + B(E)a_-(E) = 0$, so the reflection of a wave $u_E(x)$ "traveling" to the right is thus simply a wave $-[A(E)/B(E)]u_E^*(x)$ traveling to the left. After one bounce then, the wave function traveling to the left is

$$\Psi_2(x,t) = -\int_0^\infty W(E)\frac{A(E)}{B(E)}u_E^*(x)\mathrm{e}^{-\mathrm{i}Et/\hbar}\mathrm{d}E \,. \tag{33}$$

Calculating the sum of all the reflections will give

$$\sum_{i=1}^\infty \Psi_i(x,t) = \int_0^\infty W(E)\left[\sum_{i=0}^\infty \left(\frac{A(E)D(E)}{B(E)C(E)}\right)^i\right] \times \left[u_E(x) - \frac{A(E)}{B(E)}u_E^*(x)\right]\mathrm{e}^{-\mathrm{i}Et/\hbar}\mathrm{d}E \tag{34}$$

We show in the Appendix that the term in the square brackets formally approaches a sum of delta functions in a distributional sense, with peaks at the eigenenergies. Intuitively, knowing that the modulus of AD/BC must be unity, we can see that this sum will only diverge if AD/BC actually equals one. Using the result from Appendix,

$$\sum_{i=0}^\infty \left(\frac{A(E)D(E)}{B(E)C(E)}\right)^i = \sum_m |a_{+_m}|^2\delta(E - E_m) \tag{35}$$

then between x_1 and x_2, we can write

$$\begin{aligned}\sum_{i=1}^{\infty}\Psi_i(x,t) &= \int_0^{\infty} W(E)\,|a_{+_m}|^2\,\delta(E-E_m)\\ &\quad\times\left[u_E(x)-\frac{A(E)}{B(E)}u_E^*(x)\right]\mathrm{e}^{-\mathrm{i}Et/\hbar}\mathrm{d}E\\ &= \sum_m W(E_m)\,|a_{+_m}|^2\\ &\quad\times\left[u_m(x)-\frac{A(E_m)}{B(E_m)}u_m^*(x)\right]\mathrm{e}^{-\mathrm{i}E_mt/\hbar}\\ &= \sum_m W(E_m)a_{+_m}^*\phi_m(x)\mathrm{e}^{-\mathrm{i}E_mt/\hbar}\,. \end{aligned}\tag{36}$$

Note that, when the continuum description changed to a mode description, the subscripts E changed to m, so, for example, $u_m(x)$ is simply $u_E(x)$ evaluated at the m-th eigenenergy of the system. Given that the u_E functions are orthogonal, (the Appendix uses the WKB approximation to specify a set of orthogonal u_E functions) and the initial wave packet lies between x_1 and x_2,

$$W(E_m)=\int_{x_1}^{x_2}\psi(x,0)u_m^*(x)\mathrm{d}x\,,\tag{37}$$

and further, if we assume as previously that the atomic wave function is initially traveling predominantly to the right,

$$\begin{aligned}c_m &= \int_{x_1}^{x_2}\psi(x,0)\phi_m^*(x)\mathrm{d}x\\ &= \int_{x_1}^{x_2}\psi(x,0)[a_{+_m}^*u_m^*(x)+a_{-_m}^*u_m(x)]\mathrm{d}x\\ &\approx a_{+_m}^*\int_{x_1}^{x_2}\psi(x,0)u_m^*(x)\mathrm{d}x\\ &= a_{+_m}^*W(E_m)\,. \end{aligned}\tag{38}$$

By substituting (38) into (36), we find that the infinite sum of the reflected waves gives the same result for the time-dependent solution as the energy-eigenstate technique, as in (22).

When we consider the three-dimensional case, the problem becomes significantly more complicated. The major differences occur with the reflections, as unlike the one-dimensional case, where the reflection coefficients stayed constant, in three dimensions the coefficients are a function of the position of the bounce. Physically, this means the reflected wave depends on the position the atom bounced on the evanescent wave. The procedure we follow is precisely the same as for one dimension. First, in Sect. 3.2, we solve the TISE ignoring the boundary conditions, between two surfaces, (which are the analogue of the points x_1 and x_2 in the one-dimensional situation). We specifically choose these surfaces so that they are sufficiently far away from the classical turning points for the range of energies with which we are concerned, so that we can use a WKB-type approximation throughout the region between the surfaces. Second, in Sect. 3.3, we calculate the reflection conditions imposed by the boundaries at both the top and the bottom of the bounce, which corresponds to finding the A,B,C and D coefficients in the one-dimensional case. Finally, in Sect. 3.4, we combine all of the terms in the infinite sum, and calculate the time-dependent solution. In this section we introduce the time-dependent phase factor, and note that because of this, given the solution is narrowband in energy, only one of the traveling solutions, (i.e., the group of energies with solutions traveling to the left or the right after a given number of bounces) is going to contribute significantly. It is because of this simple interpretation of the stationary (i.e., constant energy, even though they may not satisfy the boundary conditions) wave functions as "traveling" that the technique used is so much more transparent than that using the energy eigenstates.

3.2 Distinguishable directions

In the regions which are sufficiently distant in the z-direction from the classical turning points, we can clearly distinguish between the atomic wave function traveling upwards and the one traveling downwards. In this region, we can use an approach analogous to Gaussian-wave optics, and hence write

$$\psi(\mathbf{r})=\phi_z^+(x,y)\mathrm{e}^{\mathrm{i}\int k(z)\mathrm{d}z}+\phi_z^-(x,y)\mathrm{e}^{-\mathrm{i}\int k(z)\mathrm{d}z}\,,\tag{39}$$

where $\phi_z^{\pm}$ are slowly varying in z, and $k(z)$ is the de Broglie wave number of the atom in the z-direction, so if (x_0,y_0) and (K_x,K_y) are the mean position and wave number of the wave function in the xy-plane for the wave function at position z, then

$$\frac{\hbar^2}{2m}\left[k(z)^2+K_x^2+K_y^2\right]+V(x_0,y_0,z)=E.\tag{40}$$

As in Gaussian-wave propagation, using the paraxial approximation, we ignore the second z derivative of the slowly varying functions $\phi_z^{\pm}$, and hence obtain a differential equation

$$\begin{aligned}&\frac{\partial^2\phi_z^{\pm}}{\partial x^2}+\frac{\partial^2\phi_z^{\pm}}{\partial y^2}\pm\mathrm{i}\frac{\partial k}{\partial z}\phi_z^{\pm}\pm2\mathrm{i}k\frac{\partial\phi_z^{\pm}}{\partial z}+K_x^2\phi_z^{\pm}+K_y^2\phi_z^{\pm}\\ &\qquad=\frac{2m}{\hbar^2}\left[V(x,y,z)-V(x_0,y_0,z)\right]\phi_z^{\pm}\,.\end{aligned}\tag{41}$$

In the region where the evanescent wave is negligible, the right-hand side evaluates to zero, so transforming to the Fourier domain (k_x,k_y) of (x,y), and solving

$$\begin{aligned}\Phi_z^{\pm}(k_x,k_y)&=\Phi_{z_0}^{\pm}(k_x,k_y)\sqrt{\frac{k(z_0)}{k(z)}}\\ &\quad\times\exp\left(\pm\mathrm{i}\int_{z_0}^{z}\mathrm{d}z\frac{K_x^2+K_y^2-k_x^2-k_y^2}{2k}\right),\end{aligned}\tag{42}$$

where

$$k(z)=\sqrt{C_z(z_{00}-z)}\,,\tag{43}$$

$$C_z=\frac{2m^2g}{\hbar^2}\,,\tag{44}$$

and z_{00} is the classical turning point at the top of the bounce. Due to the fact that the second factor in (42) does not depend on k_x or k_y, and the third is merely a phase factor, we conclude that while the atomic wave function is evolving in gravity alone, the mean wave number in the x- and

y-directions, K_x and K_y, must remain constant. It is then possible to solve the integral in the third factor, as all of the terms in the numerator do not depend on z. The wave function is hence a simple multiplication by a Gaussian in the momentum representation, or a convolution with a Gaussian in the position representation. If we assume the wave function at position z_0 to be a Gaussian form which is written as

$$\phi_z^{\pm} = A_x(z)A_y(z)\frac{\sqrt{C(z)D(z)}}{\sqrt{k(z)}} \times \exp\left[-C(z)\left(x - \frac{C_2(z)}{2}\right)^2 - D(z)\left(y - \frac{D_2(z)}{2}\right)^2\right], \quad (45)$$

where each of the functions of z : A_x, A_y, C, D, C_2, D_2, are assigned values at z_0, then we find that the solution has exactly the same form as above, with the functions of z being

$$A_{x,y}(z) = A_{x,y}(z_0) \times \exp\left[\pm \mathrm{i}\frac{K_{x,y}^2}{\sqrt{C_z}}\left(\sqrt{z_{00} - z_0} - \sqrt{z_{00} - z}\right)\right], \quad (46)$$

$$C(z)^{-1} = C(z_0)^{-1} \pm \frac{4\mathrm{i}}{\sqrt{C_z}}\left(\sqrt{z_{00} - z_0} - \sqrt{z_{00} - z}\right), \quad (47)$$

$$D(z)^{-1} = D(z_0)^{-1} \pm \frac{4\mathrm{i}}{\sqrt{C_z}}\left(\sqrt{z_{00} - z_0} - \sqrt{z_{00} - z}\right), \quad (48)$$

$$C_2(z) = C_2(z_0), \quad (49)$$

$$D_2(z) = D_2(z_0). \quad (50)$$

We note here the analogy with Gaussian-wave optics, and in particular propagation through a homogeneous medium, which would have given an equation of the form

$$C(z)^{-1} = C(z_0)^{-1} + \mathrm{i} \quad \text{const} \quad (z - z_0). \quad (51)$$

The square-root functions that we obtain for the bouncing atom, as opposed to the linear functions obtained in the homogeneous medium, are directly the result of the dependence of the wave number k on z.

In the region where the evanescent wave is non-negligible, the right-hand side does not evaluate to zero. If we assume the spread of the wave function is small compared to the characteristic length of the change of the Rabi frequency in the x- and y- directions, then for any position (x, y, z) where the wave function has non-negligible values,

$$\omega_1^2(\mathbf{r}) - \omega_1^2(x_0, y_0, z) \ll \delta^2 + \omega_1^2(x_0, y_0, z), \quad (52)$$

$$x^2 - x_0^2 \ll \frac{1}{\frac{\alpha}{2R} - \frac{1}{\omega_x^2}}, \quad (53)$$

$$y^2 - y_0^2 \ll \frac{1}{\frac{\alpha}{2R} - \frac{1}{\omega_y^2}}, \quad (54)$$

we can write

$$V(x, y, z) - V(x_0, y_0, z_0) = \frac{\hbar}{2}\left[\sqrt{\delta^2 + \omega_1^2(\mathbf{r})} - \sqrt{\delta^2 + \omega_{1_0}^2(z)}\right] + mg(z - z_0) \quad (55)$$

$$\approx \frac{\hbar}{4}\frac{d\left(\omega_1^2\right)}{\sqrt{\delta^2 + \omega_{1_0}^2(z)}} + mg(z - z_0), \quad (56)$$

where

$$\omega_{1_0}(z) = \omega_1(x_0, y_0, z). \quad (57)$$

Here, x_0 and y_0 are functions of z. Further using (53) and (54), we obtain the right-hand side of (41) as

$$\frac{2m}{\hbar^2}\left[V(x, y, z) - V(x_0, y_0, z)\right] \approx G_x(x^2 - x_0^2) + G_y(y^2 - y_0^2), \quad (58)$$

where

$$G_{x,y} = \frac{m\omega_{1_0}^2(z)}{2\hbar\sqrt{\delta^2 + \omega_{1_0}^2(z)}}\left(\frac{\alpha}{2R} - \frac{1}{\omega_{x,y}^2}\right). \quad (59)$$

Equation (41) is analytically intractable in this region, and so we substitute the form of (45) into it, thus obtaining a set of six coupled differential equations, which we solve numerically, using a Runge-Kutta algorithm. Due to the sharp decrease in the amplitude of the Rabi frequency, and hence the quasi-potential in the z-direction, the numerical integration can be completed in an extremely short time, and the atomic wave function in the x- and y-directions does not change significantly.

3.3 Indistinguishable directions

For z-positions sufficiently close to the classical turning points, at the top and the bottom of the bounce, it is impossible to distinguish the part of the wave function traveling upwards from that traveling downwards, and so we cannot use the Gaussian-optics approach considered in the previous section. Rather, we must solve the entire Schrödinger equation, identify the part of it with the wave traveling up and the part with the wave traveling down, and hence obtain the reflection coefficients. We shall consider the top and the bottom of the bounce in turn.

3.3.1 The top of the bounce. At the top of the bounce, the evanescent wave is negligible, and the potential felt by the atomic wave function is entirely due to gravity,

$$V(\mathbf{r}) = mgz. \quad (60)$$

The Schrödinger equation,

$$-\frac{\hbar^2}{2m}\left(\frac{\partial^2\Phi}{\partial x^2} + \frac{\partial^2\Phi}{\partial y^2} + \frac{\partial^2\Phi}{\partial z^2}\right) = (E - mgz)\Phi \quad (61)$$

can be solved using separation of variables, giving complex exponential functions in the x- and y-directions, and Airy functions in the z-direction. The general solution can be written as

$$\Phi(\mathbf{r}) = \int_{-\infty}^{\infty} \mathrm{d}k_x \int_{-\infty}^{\infty} \mathrm{d}k_y \, \mathrm{e}^{\mathrm{i}k_x x}\mathrm{e}^{\mathrm{i}k_y y} \times \left[A(k_x, k_y)\mathrm{Ai}(u) + B(k_x, k_y)\mathrm{Bi}(u)\right], \quad (62)$$

where

$$u = C_z^{\frac{1}{3}}(z - z_{00}), \quad (63)$$

$$z_{00} = \frac{1}{C_z}\left(\frac{2m}{\hbar^2}E - k_x^2 - k_y^2\right). \quad (64)$$

When u is large and negative, we are once again sufficiently distant from the classical turning point to distinguish between the waves traveling up or down, and we can approximate the Airy functions as

$$\mathrm{Ai}(u) \approx \frac{1}{\sqrt{\pi}} \frac{1}{\sqrt[4]{|u|}} \cos\left(\frac{2}{3}|u|^{\frac{3}{2}} - \frac{\pi}{4}\right) , \tag{65}$$

$$\mathrm{Bi}(u) \approx \frac{1}{\sqrt{\pi}} \frac{1}{\sqrt[4]{|u|}} \sin\left(\frac{2}{3}|u|^{\frac{3}{2}} - \frac{\pi}{4}\right) . \tag{66}$$

We can identify $\mathrm{Ai}(u) + \mathrm{iBi}(u)$ as the wave traveling upwards and $\mathrm{Ai}(u) - \mathrm{iBi}(u)$ as the wave traveling downwards. The (k_x, k_y) values can be interpreted here as wave numbers in the x- and y-directions, and as such we can expect the coefficients $A(k_x, k_y)$ and $B(k_x, k_y)$ to have non-negligible values only for a range of k_x and k_y values centered around the mean wave numbers K_x and K_y. Given this, for z sufficiently below the classical turning point, we can write,

$$u = C_z^{\frac{1}{3}} \left(z - z_{00}^- + \frac{\Delta\left(k_x^2\right) + \Delta\left(k_x^2\right)}{C_z}\right) , \tag{67}$$

$$|u|^{\frac{3}{2}} \approx \sqrt{C_z}(z_{00}^- - z)^{\frac{3}{2}} - \frac{3}{2}\frac{\sqrt{z_{00}^- - z}}{\sqrt{C_z}} \left[\Delta\left(k_x^2\right) + \Delta\left(k_x^2\right)\right] , \tag{68}$$

where

$$z_{00}^- = \frac{1}{C_z}\left(\frac{2m}{\hbar^2}E - K_x^2 - K_y^2\right) , \tag{69}$$

$$\Delta\left(k_{x,y}^2\right) = k_{x,y}^2 - K_{x,y}^2 , \tag{70}$$

and hence, the wave traveling upwards can be written as

$$\begin{aligned} \Phi^+(\mathbf{r}) &= \int_{-\infty}^{\infty} \mathrm{d}k_x \int_{-\infty}^{\infty} \mathrm{d}k_y \mathrm{e}^{\mathrm{i}k_x x} \mathrm{e}^{\mathrm{i}k_y y} A^+(k_x, k_y) \\ &\quad \times [\mathrm{Ai}(u) + \mathrm{iBi}(u)] \qquad (71) \\ &\approx \int_{-\infty}^{\infty} \mathrm{d}k_x \int_{-\infty}^{\infty} \mathrm{d}k_y \mathrm{e}^{\mathrm{i}k_x x} \mathrm{e}^{\mathrm{i}k_y y} \frac{A^+(k_x, k_y)}{\sqrt{\pi}\sqrt[4]{|u|}} \\ &\quad \times \exp\left\{\frac{2\mathrm{i}}{3}\sqrt{C_z}\,(z_{00}^- - z)^{\frac{3}{2}} \right. \\ &\quad \left. -\mathrm{i}\frac{\sqrt{z_{00}^- - z}}{\sqrt{C_z}} \left[\Delta\left(k_x^2\right) + \Delta\left(k_y^2\right)\right] - \frac{\mathrm{i}\pi}{4}\right\} . \qquad (72) \end{aligned}$$

We use the approximation that $\sqrt[4]{|u|} \approx \sqrt[4]{|\bar{u}|}$, where $\bar{u} = C_z^{\frac{1}{3}}(z - z_{00}^-)$, as the function is slowly varying over the range of k_x and k_y values for which $A^+(k_x, k_y)$ is non-negligible. Note that the first term in the exponential in (72) corresponds exactly to the upwards traveling wave phase factor $\mathrm{e}^{\mathrm{i}\int k(z)\mathrm{d}z}$ in (39), with the possible discrepancy of a multiplicative constant. Because of this correspondence, (72) gives a quantitative understanding of what until now has been a qualitative distinction between indistinguishable and distinguishable directions, or z-positions sufficiently close to the classical turning points. If we are at a position z where we can approximate the wave function as in (72), then we know for all positions z below this the Gaussian-wave optics approach is valid, as the first term in the exponential corresponds to the $\mathrm{e}^{\mathrm{i}\int k(z)\mathrm{d}z}$, and the remainder corresponds to $\phi_z^+(x, y)$ and is in comparison to the first term, slowly varying in z. Hence, our criterion for the validity of the Gaussian-wave optics approach is the same as for (68). For all values of k_x, k_y, where $A^+(k_x, k_y)$ is non-negligible (physically, for all non-negligible momentum components of the wave function) and a position z, the Gaussian-wave optics approach is valid if

$$\left|\frac{\Delta\left(k_x^2\right) + \Delta\left(k_y^2\right)}{C_z}\right| \ll z_{00}^- - z. \tag{73}$$

We match this solution for the upwards-traveling wave with the solution obtained using the Gaussian-optics technique,

$$\begin{aligned} \phi_z^+(x, y) &= \int_{-\infty}^{\infty} \mathrm{d}k_x \int_{-\infty}^{\infty} \mathrm{d}k_y \mathrm{e}^{\mathrm{i}k_x x} \mathrm{e}^{\mathrm{i}k_y y} \frac{A^+(k_x, k_y)}{\sqrt{\pi}\sqrt[4]{|\bar{u}|}} \\ &\quad \times \exp\left\{-\mathrm{i}\frac{\sqrt{z_{00}^- - z}}{\sqrt{C_z}} \left[\Delta\left(k_x^2\right) + \Delta\left(k_y^2\right)\right] - \frac{\mathrm{i}\pi}{4}\right\} \qquad (74) \\ &= A_x(z) A_y(z) \frac{\sqrt{C(z)D(z)}}{\sqrt{k(z)}} \\ &\quad \times \exp\left[-C(z)\left(x - \frac{C_2(z)}{2}\right)^2 - D(z)\left(y - \frac{D_2(z)}{2}\right)^2\right] , \qquad (75) \end{aligned}$$

and using the orthogonality of the complex exponentials, we solve for $A^+(k_x, k_y)$. For u large and positive, which corresponds to the positions above the classical turning point, the Airy functions can be approximated as

$$\mathrm{Ai}(u) \approx \frac{1}{2\pi} \frac{1}{\sqrt[4]{u}} \exp\left(-\frac{2}{3}u^{\frac{3}{2}}\right) , \tag{76}$$

$$\mathrm{Bi}(u) \approx \frac{1}{\pi} \frac{1}{\sqrt[4]{u}} \exp\left(\frac{2}{3}u^{\frac{3}{2}}\right) . \tag{77}$$

We wish to superpose onto the solution for the wave traveling upwards a wave function which fulfills two conditions. First, sufficiently below the classical turning point it should only be traveling downwards, and second, when superposed with the portion of the wave function traveling up, it should cancel the exponentially increasing component of the wave function above the classical turning point. It can be seen that this solution will have the same coefficients $A^+(k_x, k_y)$ as the upwards traveling wave, and have the form $\mathrm{Ai}(u) - \mathrm{iBi}(u)$, for the z-section of the separated variables solution.

$$\begin{aligned} \Phi^-(\mathbf{r}) = \int_{-\infty}^{\infty} \mathrm{d}k_x \int_{-\infty}^{\infty} \mathrm{d}k_y \;\; & \mathrm{e}^{\mathrm{i}k_x x} \mathrm{e}^{\mathrm{i}k_y y} A^+(k_x, k_y) \\ & \times [\mathrm{Ai}(u) - \mathrm{iBi}(u)] . \end{aligned} \tag{78}$$

Finally, we can evaluate the part of the wave function traveling down at position z (where z is once again sufficiently far from the classical turning point) as a function of the wave-function part traveling up. If we write both parts of the wave function in the form given in (45), with the functions of z referring to the wave traveling upwards characterized by the superscript + and referring to those traveling down with superscript $-$, then we obtain,

$$A_{x,y}^-(z) = A_{x,y}^+(z) \exp\left(-2\mathrm{i}\frac{\sqrt{z_{00}^- - z}}{\sqrt{C_z}} K_{x,y}^2 + \frac{i\pi}{4}\right) , \tag{79}$$

$$C^-(z)^{-1} = C^+(z)^{-1} + \frac{8\mathrm{i}\sqrt{z_{00}-z}}{\sqrt{C_z}}\,, \tag{80}$$

$$D^-(z)^{-1} = D^+(z)^{-1} + \frac{8\mathrm{i}\sqrt{z_{00}-z}}{\sqrt{C_z}}\,, \tag{81}$$

$$C_2^-(z) = C_2^+(z_0)\,, \tag{82}$$

$$D_2^-(z) = D_2^+(z_0)\,. \tag{83}$$

It is noted here that the method used is almost entirely analogous to the connection formulae used in the WKB-approximation scheme in one dimension, however, we have obtained the solution in three dimensions, by considering only the Airy function in the z-direction.

3.3.2 The bottom of the bounce. While the analysis of the change in the wave function at the bottom of the bounce is conceptually similar to that at the top, mathematically and physically it is significantly more complex, due to the x and y dependence of the potential felt by the atom. We first evolve the wave function using Gaussian-wave optics to a z-position sufficiently close to the classical turning point that the potential can be expanded linearly in z, and sufficiently far away that the Gaussian-wave optics approach is still valid. Using a similar expansion to that used in (52–59), but also expanding linearly in the z-direction around the classical turning point (x_0, y_0, z_0), we obtain the Schrödinger equation as

$$\frac{\partial^2\Phi}{\partial x^2} + \frac{\partial^2\Phi}{\partial y^2} + \frac{\partial^2\Phi}{\partial z^2} \approx \left[G_x(x^2 - x_0^2) + G_y(y^2 - y_0^2) - G_z(z - z_0)\right]\Phi\,, \tag{84}$$

where

$$G_z = \frac{m\omega_{1_0}^2\alpha}{\hbar\sqrt{\delta^2 + \omega_{1_0}^2}} - \frac{2m^2 g}{\hbar^2}\,, \tag{85}$$

$$G_{x,y} = \frac{m\omega_{1_0}^2}{\hbar\sqrt{\delta^2 + \omega_{1_0}^2}}\left(\frac{\alpha}{2R} - \frac{1}{\omega_{x,y}^2}\right)\,, \tag{86}$$

$$\omega_{1_0} = \omega_1(x_0, y_0, z_0)\,. \tag{87}$$

Before we consider the general solution, we shall consider a simple approximation which is valid in many situations.

If we assume that the wave function in the position representation does not change significantly in the x- and y-directions, for the evolution through the bottom of the bounce (i.e., from the initial z-position on the way downwards to the same position on the way up) then this is equivalent to assuming that the second derivative of the wave function with respect to x- and y- can be neglected in the analysis. Hence, we obtain a simple second-order differential equation in z which has the Airy functions as its solution.

$$\frac{\partial^2\Phi}{\partial z^2} = -G_z\left[z - z_0(x, y)\right]\Phi\,, \tag{88}$$

where

$$z_0(x, y) = z_0 + \frac{1}{G_z}\left[G_x(x^2 - x_0^2) + G_y(y^2 - y_0^2)\right] \tag{89}$$

and so $\Phi(\mathbf{r}) = A(x, y)\mathrm{Ai}(u) + B(x, y)\mathrm{Bi}(u)$, where $u = -C_z^{\frac{1}{3}}[z - z_0(x, y)]$. Identifying $\Phi^-(\mathbf{r}) = A^-(x, y)[\mathrm{Ai}(u) - \mathrm{iBi}(u)]$ as the wave traveling down, approximating the Airy functions as above, equating the general solution with that obtained for the wave traveling downwards using the Gaussian-optics approach, we can solve for $A^-(x, y)$. Using the same arguments as we used at the top of the bounce, we substitute $A^-(x, y)$ into $\Phi^+(\mathbf{r}) = A^-(x, y)[\mathrm{Ai}(u) + \mathrm{iBi}(u)]$, and obtain

$$C^+(z) = C^-(z) + 2\mathrm{i}\frac{G_x\sqrt{z - z_0}}{\sqrt{G_z}}\,, \tag{90}$$

$$D^+(z) = D^-(z) + 2\mathrm{i}\frac{G_y\sqrt{z - z_0}}{\sqrt{G_z}}\,, \tag{91}$$

$$C_2^+(z) = \frac{C_2^-(z)C^-(z)}{C^+(z)}\,, \tag{92}$$

$$D_2^+(z) = \frac{D_2^-(z)D^-(z)}{D^+(z)}\,, \tag{93}$$

$$A_x^+(z) = A_x^-(z)\exp\left(2\mathrm{i}\frac{G_x\sqrt{z - z_0}}{\sqrt{G_z}}x_0^2 + \frac{C^+(z)C_2^+(z)^2}{4} - \frac{\mathrm{i}\pi}{4}\right)\,, \tag{94}$$

$$A_y^+(z) = A_y^-(z)\exp\left(2\mathrm{i}\frac{G_y\sqrt{z - z_0}}{\sqrt{G_z}}y_0^2 + \frac{D^+(z)D_2^+(z)^2}{4} - \frac{\mathrm{i}\pi}{4}\right)\,, \tag{95}$$

where once again the superscript + refers to the part of the wave function traveling up, and − refers to that part traveling down. We note that, in this situation, we can show that the change of the mean wave number in the x-direction, for example, is linearly dependent on the x-position of the bounce

$$K_x^+(z) = K_x^-(z) - \frac{4G_x\sqrt{z - z_0}}{\sqrt{G_z}}x_0\,. \tag{96}$$

This is precisely the sort of relation we would expect for a lossless system where a point mass is bouncing on a hard surface which has been polished into a concave surface where the x- and y-position of the surface depend quadratically on z.

For the general solution, we must once again use separation of variables. Writing the atomic wave function as $\Phi = X(x)Y(y)Z(z)$, so that we obtain the separated differential equations as

$$\left(\frac{\partial^2}{\partial x^2} - G_x x^2\right)X_n(x) = \left(-G_x x_0^2 - a_n\right)X_n(x)\,, \tag{97}$$

$$\left(\frac{\partial^2}{\partial y^2} - G_y y^2\right)Y_m(y) = \left(-G_y y_0^2 - b_m\right)Y_m(y)\,, \tag{98}$$

$$\frac{\partial^2 Z_{nm}(z)}{\partial z^2} = \left[-G_z(z - z_0) + a_n + b_m\right]Z_{nm}(z)\,. \tag{99}$$

These equations have solutions which are parabolic cylinder functions in the x- and y-directions, and Airy functions in the z-direction. The fact, however, that the solution must be normalizable, and cannot have diverging values as x- or y- approaches positive or negative infinity, imposes a physical restriction on the $X(x)$ and $Y(y)$ functions that can be chosen, namely, those parabolic cylinder functions which are normalizable. These functions are the well-known energy eigenstates of the harmonic oscillator

$$X_n(x) = N_n^{(x)} e^{-\frac{1}{2}\alpha_x^2 x^2} H_n(\alpha_x x) , \quad (100)$$

$$Y_m(y) = N_m^{(y)} e^{-\frac{1}{2}\alpha_y^2 y^2} H_m(\alpha_y y) , \quad (101)$$

$$Z_{nm} = A_{nm}\mathrm{Ai}(u_{nm}) + B_{nm}\mathrm{Bi}(u_{nm}) , \quad (102)$$

where

$$N_p^{(x,y)} = \sqrt{\frac{\alpha_{x,y}}{2^p p!\sqrt{\pi}}} \quad (103)$$

and $\alpha_{x,y} = \sqrt[4]{G_{x,y}}$, $u_{nm} = -\sqrt{G_z}[(z-\bar{z}_0)+\Delta(a_n)+\Delta(b_m)]$, where $\bar{z}_0 = z_0 + (\bar{a}+\bar{b})/G_z$, $\bar{a} = a_n + \Delta(a_n)$ and $\bar{b} = b_m + \Delta(b_m)$. We can further write $a_n = \alpha_x^2(2n+1) - G_x x_0^2$ and $b_m = \alpha_y^2(2m+1) - G_y y_0^2$ due to the restriction on the possible eigenvalues of (97) and (98). H_n refers to the n-th Hermite polynomial, and n and m are non-negative integers. The general solution for the wave traveling downwards is

$$\Phi^-(\mathbf{r}) = \sum_{n,m=0}^{\infty} A_{nm} N_n^{(x)} e^{-\frac{1}{2}\alpha_x^2 x^2} H_n(\alpha_x x) N_m^{(y)} e^{-\frac{1}{2}\alpha_y^2 y^2} \times H_m(\alpha_y y)[\mathrm{Ai}(u_{nm}) - \mathrm{iBi}(u_{nm})] . \quad (104)$$

Following the now familiar procedure, and using the Gauss transform of a Hermite polynomial [12],

$$G_x^{\mu}[H_n(y)] = (1-2\mu)^{\frac{n}{2}} H_n\left(\frac{x}{\sqrt{1-2\mu}}\right) , \quad (105)$$

where

$$G_x^{\mu}[F(y)] = \frac{1}{2\pi\mu}\int_{\infty}^{\infty} F(y)\exp\left(-\frac{(x-y)^2}{2\mu}\right) , \quad (106)$$

and Mehler's formula [12]

$$\sum_{n=0}^{\infty} \frac{\left(\frac{z}{2}\right)^n}{n!} H_n(x)\, H_m(y) = \frac{1}{\sqrt{1-z^2}} \exp\left(\frac{2xy(x^2+y^2)z^2}{1-z^2}\right) , \quad (107)$$

we obtain the solution for the part of the upcoming wave function as a function of the downwards-going wave function. These solutions are rather bulky and are not reproduced here.

We note that there are two intermediate approximations between these two solutions, which involve removing the constant momenta in the x- and y-directions by creating a new function $\Phi_{x,y}(z) = \Phi(\mathbf{r})e^{-\mathrm{i}K_x x - \mathrm{i}K_y y}$, and ignoring first all derivatives, and second, only the second derivative in z. These approximations would be particularly useful in glancing-incidence problems off the evanescent wave.

3.4 Time dependence

To this point in our discussion of the quantum model, we have been obtaining stationary solutions in the region between the classical turning points, and reflection coefficients at the boundaries. While we have described part of the wave function as traveling upwards, and the other part as traveling downwards, we cannot characterize the wave as "traveling" in any time-dependent sense. What is in fact meant by these statements is that, for the upwards traveling part of the wave function, the phase at some position z is greater than the phase at position z_0, where $z > z_0$, and similarly, for the part of the wave function traveling downwards, the phase is greater for lower z-positions. Following further the line of reasoning in Sect. 3.1, we shall construct an infinite sum of wave functions multiplied by their time-dependent phase functions. Our first assumption is that the solution is narrow-band, and only depends on a small range of energies. Mathematically, this is assuming that $F(\nu)$ has non-negligible values for only a small range of frequencies, which are all similar to the central frequency ν_0. Further, we assume that the x- and y-dependence of each of the stationary solutions is the same as the x- and y-dependence for the central frequency. The general stationary solution $\psi_\nu(\mathbf{r})$, can be written as a sum of Gaussian forms which represent the x- and y-dependence of the solution,

$$\phi_z^{(n)}(\nu) = A_x^{(n)}(\nu,z)A_y^{(n)}(\nu,z)\frac{\sqrt{C^{(n)}(\nu,z)D^{(n)}(\nu,z)}}{\sqrt{k^{(n)}(\nu,z)}} \times \exp\left[-C^{(n)}(\nu,z)\left(x - \frac{C_2^{(n)}(\nu,z)}{2}\right)^2 - D^{(n)}(\nu,z)\left(y - \frac{D_2^{(n)}(\nu,z)}{2}\right)^2\right] , \quad (108)$$

multiplied by phase factors $e^{\mathrm{i}I^{(n)}(\nu,z)}$ which correspond to the $e^{\pm\mathrm{i}\int k^{(n)}(\nu,z)\mathrm{d}z}$ factors in (39). The successive evolutions from classical turning point to classical turning point in both directions are referenced by the index n, and each of the functions of z is itself different for different n values. Noting the above approximation that the x- and y- dependence is the same as for the central frequency, we can write

$$\Psi(\mathbf{r},t) = \sum_n \phi_z^n(\nu_0)\int_{-\infty}^{\infty} F(\nu)e^{\mathrm{i}I^{(n)}(\nu,z)}e^{-\mathrm{i}2\pi\nu t}\mathrm{d}\nu . \quad (109)$$

For a given time t, it is only values of the central frequency phase $I^{(n)}(\nu_0,z)$, where $I^{(n)}(\nu_0,z) \approx 2\pi\nu_0 t$, that will contribute significantly to the total wave function, as different values of the phase will cause the complex exponential functions in the integrand to be sufficiently oscillatory over the range of frequencies for which $F(\nu)$ is non negligible that the total contribution will average to zero. As the phase is always increasing, only a single Gaussian form, (or two near the classical turning points) will contribute to the total wave function at any one time.

3.4.1 Distinguishable directions. If initially we assume that only one Gaussian form is contributing, which is equivalent to saying that the upwards and downwards traveling waves are distinguishable, we write

$$\Psi(\mathbf{r},t) = \phi_z^{(n)}(\nu_0)\int_{-\infty}^{\infty} F(\nu)e^{\mathrm{i}I^{(n)}(\nu,z)}e^{-\mathrm{i}2\pi\nu t}\mathrm{d}\nu , \quad (110)$$

where, which Gaussian form $\phi_z^{(n)}(\nu_0)$ is chosen, depends on if the corresponding phase $I^{(n)}(\nu_0,z)$ has a value for some z between the classical turning points equal to $2\pi\nu_0 t$. In the following, for simplicity of notation, we shall remove the $\phi_z^n(\nu_0)$, where the remainder of the general solution is

described by $f(z,t)$. We expand $I^{(n)}(\nu,z)$ to second order in a Taylor series around ν_0,

$$I^{(n)}(\nu,z) = I^{(n)}(\nu_0,z) + a^{(n)}(z)(\nu-\nu_0) + b^{(n)}(z)(\nu-\nu_0)^2 \,. \tag{111}$$

Writing the initial distribution in time at some position z_0 due to a single transition through that z-position (i.e., not including any of the transitions through that position due to the bounces), as

$$f(z_0,t) = m(t)\exp\left[\mathrm{i}I^{(n)}(\nu_0,z_0) - \mathrm{i}2\pi\nu_0 t\right] \,. \tag{112}$$

We can use (110) evaluated at $z = z_0$ to find the relationship between $F(\nu)$ and $m(t)$, and substitute this relation back into (110) to find the general time-dependent solution:

$$f(z,t) = (m * q)\left(t + \frac{\Delta a^{(n)}(z)}{2\pi}\right) \times \exp\left[\mathrm{i}I^{(n)}(\nu_0,z_0) - \mathrm{i}2\pi\nu_0 t\right] \,, \tag{113}$$

where

$$q(t) = \sqrt{\frac{\pi}{\mathrm{i}\Delta b^{(n)}(z)}}\exp\left(\frac{\mathrm{i}\pi^2 t^2}{\Delta b^{(n)}(z)}\right) \tag{114}$$

and $\Delta a^{(n)}(z) = a^{(n)}(z) - a^{(n)}(z_0)$, $\Delta b^{(n)}(z) = b^{(n)}(z) - b^{(n)}(z_0)$. If we assume the initial distribution in time $m(t)$ is Gaussian, we can solve for $f(z,t)$ analytically, obtaining a general solution of the form

$$f(z,t) = A\frac{\sqrt{B^{(n)}(z)}}{\sqrt{B^{(n)}(z_0)}}\exp\left[B^{(n)}(z)\left(t - \frac{B_2^{(n)}(z)}{2}\right)^2 + \mathrm{i}\Delta I^{(n)}(\nu_0,z) - \mathrm{i}2\pi\nu_0 t\right] \,, \tag{115}$$

where

$$B^{(n)}(z)^{-1} = B^{(n)}(z_0)^{-1} + \mathrm{i}\frac{\Delta b^{(n)}(z)}{\pi^2} \,, \tag{116}$$

$$B_2^{(n)}(z) = B_2^{(n)}(z_0) - \frac{\Delta a^{(n)}(z)}{\pi} \,, \tag{117}$$

$\Delta I^{(n)}(\nu_0,z) = I^{(n)}(\nu_0,z) - I^{(n)}(\nu_0,z_0)$ and A is a normalization constant. When the evanescent wave is negligible, $I(\nu_0,z_0)$, and hence $a^{(n)}(z)$ and $b^{(n)}(z)$ can be solved analytically, we obtain

$$B^{(n)}(z)^{-1} = B^{(n)}(z_0)^{-1} \pm \mathrm{i}\frac{2}{g}\left(\frac{1}{k^{(n)}(z)} - \frac{1}{k^{(n)}(z_0)}\right) \,, \tag{118}$$

$$B_2^{(n)}(z) = B_2^{(n)}(z_0) \mp \frac{2\hbar}{mg}[k^{(n)}(z) - k^{(n)}(z_0)] \,. \tag{119}$$

When the evanescent wave is not negligible, $I^{(n)}(\nu,z)$ cannot be solved analytically, but the result can be obtained by a simple numerical integration.

$$B^{(n)}(z)^{-1} = B^{(n)}(z_0)^{-1} \pm \mathrm{i}\left(\frac{m}{\hbar}\right)^2\int_{z_0}^{z}\frac{\mathrm{d}z}{k^{(n)}(z)^3} \,, \tag{120}$$

$$B_2^{(n)}(z) = B_2^{(n)}(z_0) \mp \frac{2m}{\hbar}\int_{z_0}^{z}\frac{\mathrm{d}z}{k^{(n)}(z)} \,. \tag{121}$$

3.4.2 Indistinguishable directions. We shall treat the top of the bounce, and note that the bottom of the bounce is exactly analogous. Around the region of the classical turning point at the top of the bounce, we know from (71) and (78) that we can write the stationary solution as

$$\Phi(\mathbf{r}) = \int_{-\infty}^{\infty}\mathrm{d}k_x\int_{-\infty}^{\infty}\mathrm{d}k_y\mathrm{e}^{\mathrm{i}k_x x}\mathrm{e}^{\mathrm{i}k_y y}A^{+}(k_x,k_y) \times\{[\mathrm{Ai}(u) + \mathrm{iBi}(u)] + [\mathrm{Ai}(u) - \mathrm{iBi}(u)]\} \,, \tag{122}$$

and at a position z sufficiently below the classical turning point, we can write

$$\Phi(\mathbf{r}) = \int_{-\infty}^{\infty}\mathrm{d}k_x\int_{-\infty}^{\infty}\mathrm{d}k_y\mathrm{e}^{\mathrm{i}k_x x}\mathrm{e}^{\mathrm{i}k_y y}\frac{A^{+}(k_x,k_y)}{\sqrt{\pi}\sqrt[4]{|\bar{u}|}} \times\exp\left(\mathrm{i}\frac{2}{3}|u|^{\frac{3}{2}} - \frac{\mathrm{i}\pi}{4}\right) + \int_{-\infty}^{\infty}\mathrm{d}k_x\int_{-\infty}^{\infty}\mathrm{d}k_y\mathrm{e}^{\mathrm{i}k_x x}\mathrm{e}^{\mathrm{i}k_y y}\frac{A^{+}(k_x,k_y)}{\sqrt{\pi}\sqrt[4]{|\bar{u}|}} \times\exp\left(-\mathrm{i}\frac{2}{3}|u|^{\frac{3}{2}} + \frac{\mathrm{i}\pi}{4}\right) \,, \tag{123}$$

where $|u|^{\frac{3}{2}}$ is given in (68), and we identify the first term with the wave traveling upwards, and the second term with the wave traveling downwards. Both, the second term in the approximation of $|u|^{\frac{3}{2}}$ and the $\pi/4$ phase shift were taken into account in the x- and y-dependence of the atom, and we have assumed that this dependence is the same for all non-negligible frequencies. We can hence write the general time-dependent solution as

$$\Psi(\mathbf{r},t) = \phi_z^{(n)}(\nu_0)\int_{-\infty}^{\infty}F(\nu)\mathrm{e}^{\mathrm{i}I^{(n)}(\nu,z)}\mathrm{e}^{-\mathrm{i}2\pi\nu t}\mathrm{d}\nu + \phi_z^{(n+1)}(\nu_0)\int_{-\infty}^{\infty}F(\nu)\mathrm{e}^{\mathrm{i}I^{(n+1)}(\nu,z)}\mathrm{e}^{-\mathrm{i}2\pi\nu t}\mathrm{d}\nu \,, \tag{124}$$

where

$$I^{(n)}(\nu,z) = \frac{2}{3}\sqrt{C_z}\,(z_{00}^{-} - z)^{\frac{3}{2}} \,, \tag{125}$$

$$I^{(n+1)}(\nu,z) = -\frac{2}{3}\sqrt{C_z}\,(z_{00}^{-} - z)^{\frac{3}{2}} \,. \tag{126}$$

$\phi_z^{(n)}(\nu_0)$ refers to the Gaussian form of the wave traveling upwards, and $\phi_z^{(n+1)}(\nu_0)$ to that traveling downwards. We once again neglect these terms for notational simplicity, writing the wave function part due to the upwards-going wave as

$$f(z_0,t) = m(t)\exp\left[\mathrm{i}I^{(n)}(\nu_0,z_0) - \mathrm{i}2\pi\nu_0 t\right] \,. \tag{127}$$

Repeating the procedure of the previous section, by expanding $I^{(n,n+1)}(\nu,z)$ in a Taylor series to second order around ν_0, finding the relation between $m(t)$ and $F(\nu)$ using the first term in (124), and then using this relation to solve for the wave function traveling downwards in terms of $m(t)$, we find

$$f^{-}(z,t) = (m * q)\left[t - \frac{4m}{\hbar C_z}k(z)\right] \times\exp\left[\mathrm{i}I^{(n)}(\nu_0,z_0) - \mathrm{i}2\pi\nu_0 t\right] \,, \tag{128}$$

where

$$q(t) = \sqrt{-\mathrm{i}\frac{\hbar^2 C_z k^{(n)}(z)}{8m^2\pi}}\exp\left(\mathrm{i}\frac{\hbar^2 C_z k^{(n)}(z)}{8m^2}t^2\right) . \quad (129)$$

Defining $m(t)$ as a Gaussian form allows us to solve for the wave function traveling down analytically. Using the same general form as given in (115), with + superscripts denoting the upward (or n) evolution, and $-$ superscripts denoting the downward (or $n+1$) evolution

$$B^-(z)^{-1} = B^+(z)^{-1} + \mathrm{i}\frac{4}{g}\frac{1}{k(z)} , \quad (130)$$

$$B_2^-(z) = B_2^+(z) + \frac{2\hbar}{mg}k(z) . \quad (131)$$

3.5 Discussion

Using the quantum model, the information that we obtain over and above the classical model is about the spreading of the atomic wave function in space and time. It can be seen from Figs. 4 and 5 that the mean motion in the stable gravitational cavity is exactly similar to that, obtained for a classical model. The major difference in the formulation of the theory is that, while the classical model has time as the independent variable, in the quantum model the vertical position z and the bounce number n are independent. In the quantum model, we cannot obtain information on the evolution of the wave function near the classical turning points, without summing together a large number of slightly different Airy functions. This is why the top and bottom of the bounces in Fig. 4 has been chopped. Ignoring such irrelevant details as this, however, we note that the mean position of the wave function evolves similarly to a lossless system where a mass is bouncing on a hard concave, quadratically shaped surface. The height to which it bounces depends on how fast the atom is traveling in the x- and y-directions, so that energy is conserved and, as it bounces up and down in the z-direction (Fig. 4), it oscillates from side to side in the x- and y-directions (Fig. 5). (Note that the y-direction plots are omitted as they are similar to those in the x-direction). In-between each of the interactions with the evanescent wave at the bottom of the bounce, the mean momentum of the wave function remains constant.

The spread in the x-position (Fig. 6) breathes in and out at twice the frequency of the oscillations of the mean x–position, such that it is broadest at the center of the mirror, and narrowest at the edges. This is somewhat analogous to a Gaussian wave function oscillating in a quadratic potential. We note that the oscillations of the standard deviation are not caused by any intrinsical quantum feature of the system, but is rather due to a classical-type phenomenon. To show this, we turned off the spontaneous emission in our semi-classical program, and started the system with distributions in position and velocity the same as for the probabilistic distributions of the atomic wave function. We obtain precisely the same plot for the spread in the classical distribution as we did using the TDSE.

The last feature of interest with respect to the standard deviation in the x-direction, is the fact that the maximum spread always occurs precisely at a bounce, while the minimum, except for rare coincidental situations, almost never

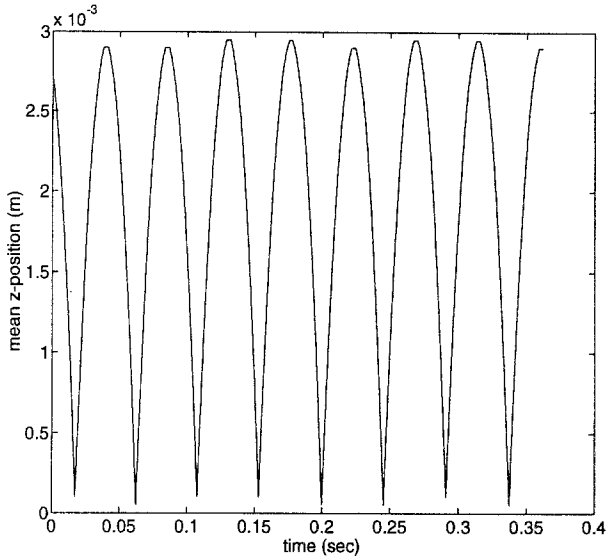

Fig. 4. Plot of the z-position of the atomic wave function vs the mean time it travels through that position. Parameters used are the same as for the classical simulation except for $\omega_{1_{max}} = 10 \times 10^9 s^{-1}$, $\omega_x = \omega_y = 1$ mm and the spontaneous emission rate $\Gamma = 0$, as no spontaneous emissions occur. Initial conditions for the atomic wave function are $B = 2.5 \times 10^9$, $B_2 = 0$, $C = D = 2.22 \times 10^{11}$, $C_2 = D_2 = 2.1 \times 10^{-3} - \mathrm{i}5.4 \times 10^{-6}$, $z_0 = 2.75$ mm, and $(E_0/\hbar) = (m/\hbar)gz_{00}$, where $z_{00} = 3$ mm. The following Figs. 5–8 were obtained using the same parameters

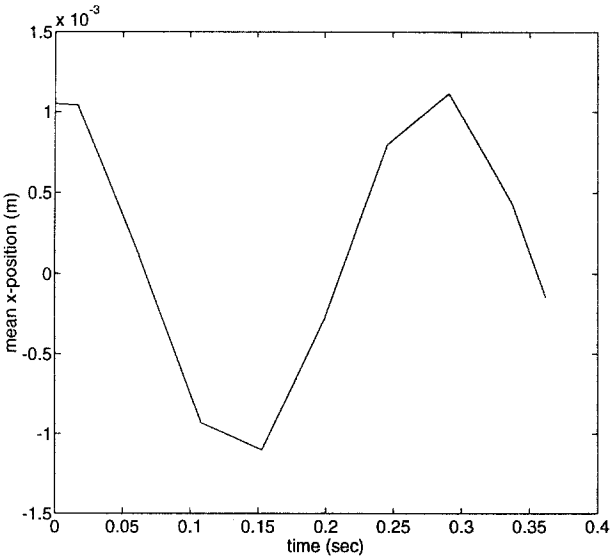

Fig. 5. Plot of mean x-position of the atomic wave function through particular z-positions vs the mean time it travels through those positions

does. This feature can be seen in the acute angular nature of the maxima and the curved minima. To understand this, we consider the imaginary part of the complex variable $C(z)^{-1}$. It can be seen in both (47) and (80) that, while evolving in gravity, this parameter is always increasing, while the real part remains constant. Noting that the standard deviation in the x-direction is $\sigma_x = 1/\sqrt{2\mathrm{Re}(C)}$, we see that if this parameter $\mathrm{Im}[C(z)^{-1}]$ is negative, the standard deviation in the x-direction will be decreasing with time, while if $\mathrm{Im}[C(z)^{-1}]$ is positive, then it shall be increasing. The only time when this parameter can become negative is when it interacts with the evanescent wave, and it follows that this

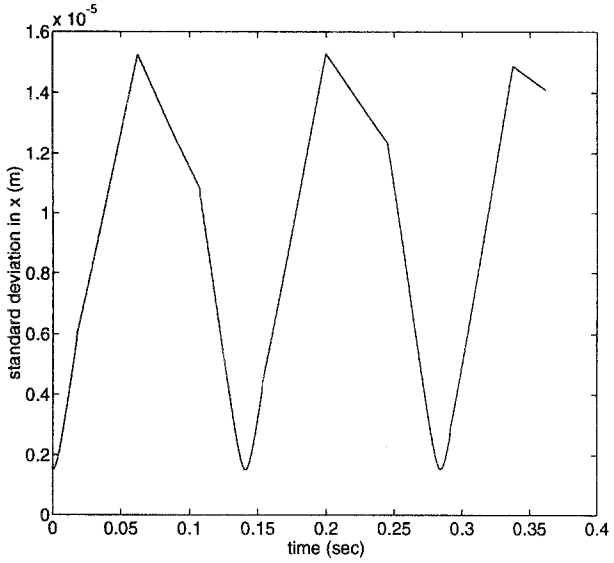

Fig. 6. Plot of the standard deviation in the x-distribution of the atomic wave function at particular z-positions vs the mean time the wave function travels through those positions

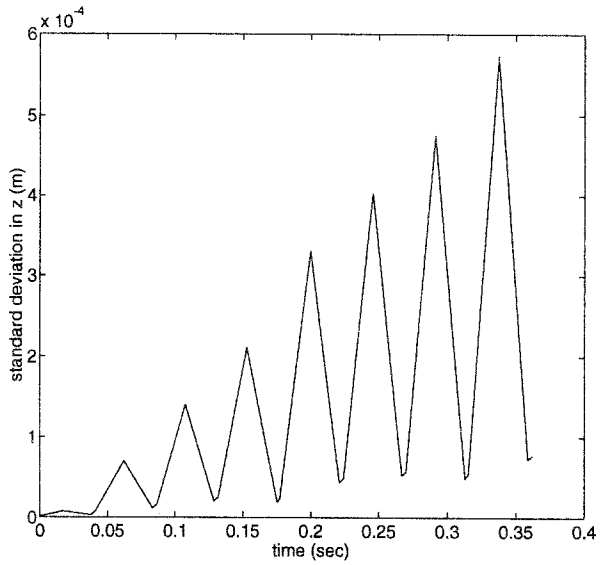

Fig. 7. Plot of the standard deviation in the z-distribution vs time, where we have assumed that the acceleration of the wave function in the time it takes to go past any particular point is negligible

is similarly the only time when the spread in the x-direction can change from increasing to decreasing, that is, the spread is maximum. We see also that the curved minima occur similarly to the waist in a laser, as the parameter $\mathrm{Im}[C(z)^{-1}]$ increases gradually from negative, through zero, to positive, causing $\mathrm{Re}[C(z)]$ to gradually obtain its maximum value. Further, if we use the simplest approximation at the bottom of the bounce, where the spread does not change over the period of the bounce (the complicated expressions give the same physical results with more mathematical complexity), and observe the behavior of the parameter $\mathrm{Im}[C(z)^{-1}]$,

$$\mathrm{Im}[C^{+}(z)^{-1}] = -\frac{\mathrm{Im}[C^{-}(z)] + \frac{2G_x\sqrt{z-z_0}}{\sqrt{G_z}}}{\mathrm{Re}[C^{-}(z)]^2 + \left\{\mathrm{Im}[C^{-}(z)] + \frac{2G_x\sqrt{z-z_0}}{\sqrt{G_z}}\right\}^2}, \qquad (132)$$

we see that the maximum change in the parameter occurs when $\mathrm{Re}[C^{-}(z)]$ is small, or σ_x is large. This has the simple physical interpretation that the more spread the wave function is, the more it feels the curvature of the mirror, and hence, it will have more of a tendency to reduce its spread in the x-direction. So there are two competing physical processes. First there is the natural tendency of the atomic wave function to disperse, and second, there are the bounces at the evanescent-wave mirror, which either decrease the rapidity of the spreading, change the spreading to contracting, or increase the rapidity of the contracting.

As z is the independent variable, it is not possible to write the distribution in z as a Gaussian form. Physically, this is attributed to the fact that we are writing the distribution in t as a Gaussian form, and hence acceleration will cause a distortion in the z-distribution from a Gaussian form. If we assume the acceleration of the wave packet over the period of time t it goes past a z-position z_0 is small $[B(z) \approx B(z_0)$ around z_0 and expand $B_2(z)$ linearly in z around $z_0]$, we can write the atomic wave function as a Gaussian in z, and hence, plot the spread in the z-position vs time (Fig. 7). This plot is dominated by the dependence on velocity. As the atom bounces, it is changing its velocity in the z-direction, and for a given spread in time, if the atom is traveling faster, it must have a broader spread in the z-direction. We can see in Fig. 7, however, that as well as this spreading due to velocity changes, causing the rapid oscillations, there is an overall tendency to spread out the atom, as the maximum spread, which occurs just before the atom enters and just after it leaves the evanescent wave, is itself increasing with time. To observe this feature, it is more convenient to observe the spread in time.

To obtain Fig. 8, we chose many z-positions and recorded the mean and the standard deviation of the time that the atomic wave function travels through that z-position for each successive bounce, and plotted the latter vs the former. We see that during the bounces, and at the bottom of the bounce in the evanescent wave, the spreading in time is relatively small; however, a large increase of the spread in time occurs at the top of the bounce. This result is consistent with our approximations, as when we used the slowly varying envelope (paraxial) approximation, in the regions between the classical turning points, the spreading was small, while at the top of the bounce, when the spreading was large, we had included all the terms and, in particular, the second-order derivative with respect to z. The features of Fig. 8 can be explained via the results of quadratic dispersion theory. We are multiplying the frequency spectrum by two factors that depend on ν. The first is a complex exponential $e^{ia(\nu-\nu_0)}$ which simply shifts the distribution in time. The second is the exponential of a complex quadratic term $e^{ib(\nu-\nu_0)^2}$. For frequencies ν where $b(\nu-\nu_0)^2 \gg 1$, the exponential will be oscillating rapidly in frequency space, while around ν_0 it will be oscillating slowly. Hence, as b increases, it will narrow the frequency spectrum around ν_0, with the consequence that the distribution in time will be broadened. This is a standard result in quadratic dispersion theory. In the regions where the direction is distinguishable,

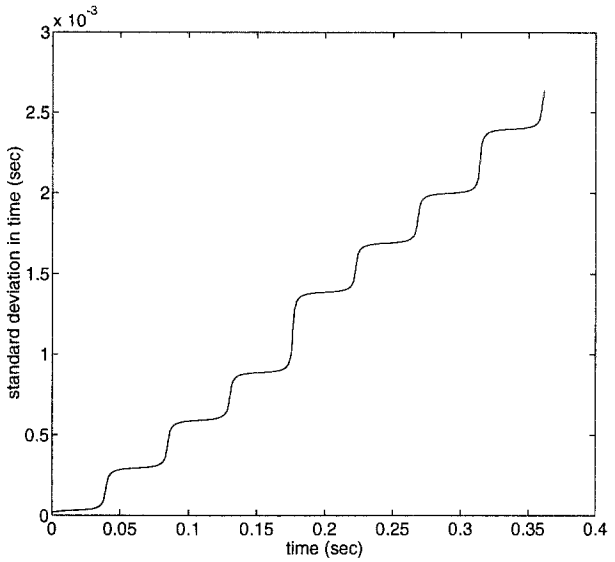

Fig. 8. Plot of the standard deviation in the time distribution of the atomic wave function at particular z-positions vs the mean time the wave function travels through those positions

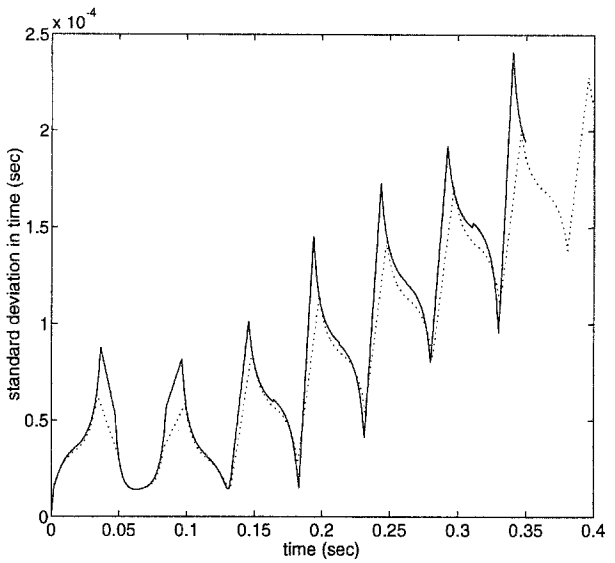

Fig. 9. Plot of the standard deviation in the time distribution of the classical statistical atomic distribution through particular z-positions vs the mean time the atomic distribution traveled through those positions. Here, the initial velocity and position distribution was chosen to correspond exactly to the probability distribution for the atomic wave function in the quantum simulation, assuming that the acceleration in the time period that the wave function went past the initial z-position $z_0 = 2.75$ mm was negligible. The *solid plot* is for a classical numerical simulation in three dimensions, while the *dotted plot* shows the analytical result for a simplified one-dimensional potential

$$b(z) = \frac{1}{2}\left.\frac{\partial^2 I^{(n)}(\nu, z)}{\partial \nu^2}\right|_{\nu=\nu_0} = \pm\frac{2\pi^2 m^2}{\hbar^2}\int_{z_0}^{z}\frac{\mathrm{d}z}{k^{(n)}(z)^3} \tag{133}$$

and at the top of the bounce

$$b^-(z) = b^+(z) + \frac{8\pi^2 m^2}{C_z \hbar^2}\frac{1}{k(z)} \tag{134}$$

with the bottom of the bounce being similar. $b(z)$ is always increasing with time, so the frequency spectrum is always narrowing, and the distribution in time broadening. Because $k(z)$ approaches zero near the classical turning points, we find the maximum spreading in these regions; however the spreading is much greater at the top of the bounce than at the bottom. Mathematically, the reason for this is that $|G_z| \gg |C_z|$, the gradient of the potential at the classical turning points. Physically, we see that it depends on the amount of time the atomic wave function spends in regions where it has a small wave number. For small gradients, such as occur at the top of the bounce, there is only a small force on the atom, and hence, a relatively large period of time is spent where the atom has a small wave number, and the consequent spreading is large. For large gradients, as occur in the evanescent wave, the force on the atom is correspondingly large, the atom spends only a short period of time with a small wave number, and the spreading is relatively small. The limiting case in this situation is where the gradient is infinite, due to a potential wall, and there is no consequent spreading of the atom.

Comparing the spreading in time with that for the classical simulation, as we did for the standard deviation in the x-distribution, there are significant discrepancies. The solid plot in Fig. 9 shows the classical simulation of the spread in time vs mean time, for a group of particles with the same distribution as for the quantum simulation. Similarly to the quantum plot, the overall tendency is for the distribution to broaden in time, however the magnitude of the spreading is significantly less. Perhaps the most striking feature of the plot is that the distribution contracts in time during its free evolution between the classical turning points. Initially, the atomic distribution broadens in free evolution; however, after a few bounces the spreading settles down to a pattern of increasing at the top of the bounce, and decreasing during the free evolution, with a small change at the evanescent potential. We understand the contraction of the standard deviation in time as being due to the sorting influence of the potential. As the atoms approach the upper classical turning point, those that have the greatest energies will travel to the highest points, while those with lowest energies will not travel as far, and hence, we obtain a consequent sorting, with the atoms that have the lowest energies, and hence, will achieve the lowest velocities at the lowest z-positions, and those atoms that will achieve relatively high velocities are at large z-positions. As the atoms accelerate from these positions down under gravity, those with large energies will catch up to those with small energies, and hence, we obtain a reduction in the spread in time. The potential gradient acts as an energy "chooser" so that atoms with high energies are spatially separated from those with low energies. The overall effect is still a spreading in time, but as the atomic distribution continues its evolution, the standard deviation in time is reduced.

To verify this interpretation, we considered a one-dimensional situation where the atomic distribution was initially in an uncorrelated Gaussian of energy and time. The potential of the system was

$$V(z) = \begin{cases} mgz & z > 0 \\ \infty & z \leq 0 \end{cases} , \tag{135}$$

where the independent variables were the bounce number n and the vertical position z. Using this idealized version of the stable gravitational cavity, we found the time t that an atom passed through a position z on bounce number n, as a function of its initial energy and time at position z_0 and bounce number $n = 0$, and hence, analytically determined the mean and standard deviation of the time distribution of the atom through the positions and bounce numbers. This standard deviation vs the mean of the time distribution is shown in the dotted plot of Fig. 9, and is seen to be extremely similar to the upper plot, with the exception of the small discrepancies due to the non-infinite gradient of the quasi-potential caused by the evanescent wave. Certainly, the qualitative character of the plots, with the atomic distribution initially spreading, and then being gradually sorted by the gradient is precisely the same, and we can conclude that in the three-dimensional case, it is similarly the "sorting" of the gradient that is causing the contraction of the distribution of the atoms.

We have found that in the x- and y-directions, both the mean and the standard deviation of the Gaussian wave packet can be analyzed correctly as a statistical distribution of atoms; however, in the z-direction, while the mean behavior is similar, the spreading in the quantum situation is much greater than that found from the statistical classical distribution, and hence, representing the distribution of a number of bouncing atoms by a classical distribution, where only the mean position and momentum for a great number of atoms is determined, will not adequately represent the actual nature of the spreading in the z-direction.

Appendix

Proof of (35)

In this Appendix, we wish to show the infinite sum in (34) can be evaluated as a sum of delta functions, peaked at the eigenenergies E_m, and to determine the coefficients for each of these energies. Initially, it will be useful to prove the following result.

$$\sum_{n=0}^{\infty} \left(e^{i\theta(E)}\right)^n = \sum_m d_m \delta(E - E_m) , \tag{A.1}$$

where

$$\theta(E_m) = 2m\pi , \tag{A.2}$$

$$d_m = \frac{2\pi}{\theta'(E_m)} , \tag{A.3}$$

and we have assumed $\theta'(E_m) \neq 0$. In a distributional sense, as $N \to \infty$, the partial sum

$$\sum_{n=0}^{N} \left(e^{i\theta(E)}\right)^n = \frac{e^{i\theta(E)N/2}}{e^{i\theta(E)/2}} \frac{\sin[\theta(E)N]}{\sin[\theta(E)]} \tag{A.4}$$

tends to zero except when $\sin[\theta(E)] = 0$. Expanding to first order around one of these values, E_m gives

$$\theta(E) \approx 2\pi m + \theta'(E_m)(E - E_m) . \tag{A.5}$$

The partial sum for values of E around E_m is then

$$\sum_{n=0}^{N} \left(e^{i\theta(E)}\right)^n = \frac{e^{i\theta'(E_m)(E-E_m)N/2}}{e^{i\theta'(E_m)(E-E_m)/2}} \frac{\sin[\theta'(E_m)(E - E_m)N]}{\sin[\theta'(E_m)(E - E_m)]} , \tag{A.6}$$

which tends to a delta function, $[2\pi/\theta'(E_m)]\delta(E - E_m)$, as $N \to \infty$.

As $|AD/BC| = 1$, we identify $AD/BC = e^{i\theta}$, and we can write the infinite sum in (34) as a sum of delta functions, which have peaks at energies where $AD/BC = 1$, which is precisely the same condition as for the eigenenergies. So

$$\sum_{i=0}^{\infty} \left(\frac{A(E)D(E)}{B(E)C(E)}\right)^i = \sum_m \frac{2\pi}{\theta'(E_m)} \delta(E - E_m) , \tag{A.7}$$

where E_m are the eigenenergies, and

$$\theta'(E) = \frac{\partial}{\partial E} \arg\left(\frac{A(E)D(E)}{B(E)C(E)}\right) . \tag{A.8}$$

Having shown that the initial infinite sum can be written as a sum of delta functions peaked at the eigenenergies, we now need only determine the coefficients of the delta functions for each of these eigenenergies. To do this, we assume the range of energies with which we are concerned, and the potential is of a form that we can use the WKB approximation, and hence, obtain an analytic form for the wave functions between the two points x_1 and x_2 chosen sufficiently far away from the range of classical turning points, and between them for the given energy spread. Neglecting for the moment the boundary conditions, we can write the WKB solutions as

$$\phi^{\pm}_{\mathrm{WKB}}(x; E) = A \frac{\exp\left[\pm \frac{i}{\hbar} \int_0^x k(\xi) d\xi\right]}{\sqrt{|k(x)|}} = A \frac{\exp[\pm i\Phi(x; E)]}{\sqrt{|k(x)|}} , \tag{A.9}$$

with $k(x)$ as defined in (30), and the general solution as a linear superposition of the WKB solutions

$$\Psi_E(x) = a_+(E)\phi^+_{\mathrm{WKB}}(x; E) + a_-(E)\phi^-_{\mathrm{WKB}}(x; E) = 2\mathrm{Re}\left[a_+\phi^+_{\mathrm{WKB}}(x; E)\right] \tag{A.10}$$

Note that $a_+ = a^*_-$, as the general solution is real.

If we consider one-sided solutions, which satisfy the boundary conditions at only the right-hand side, thus retaining a continuum of energy eigenstates, the connection formula for the right-hand barrier requires the phase of the energy eigenstate at $x_b(E)$ (the classical turning point for energy E at the right-hand barrier) to be $\pi/4$. $\Psi_E(x)$ should thus be of the form $\cos[\Phi(x; E) - \Phi(x_b; E) + \pi/4]$. We note here that, while the amplitude of the WKB solution diverges at the classical turning point, the phase does not and can be evaluated to x_b. We know then that the argument of a_+ for an eigenstate satisfying the boundary conditions at the right-hand barrier only is

$$\arg(a_+) = \frac{\pi}{4} - \Phi(x_b; E) . \tag{A.11}$$

Since $a_+ = a_-^*$, and as we have already shown in Sect. 3.1, $(A/B) = -(a_-/a_+)$, we obtain

$$\arg\left(\frac{A}{B}\right) = \pi - \arg(a_+) = \frac{\pi}{2} + 2\Phi(x_b; E) . \quad (A.12)$$

Using a similar argument for solutions which only satisfy the boundary conditions at the left barrier, which has a classical turning point $x_a(E)$, we get

$$\arg\left(\frac{D}{C}\right) = \frac{\pi}{2} - 2\Phi(x_a; E) . \quad (A.13)$$

This gives a physical interpretation of $\arg(AD/BC)$ as the total change in phase in a round trip between the classical turning points. We also rederive the quantization condition used in the "old" quantum theory, as the condition for an energy eigenstate, $\arg(AD/BC) = 2m\pi$ implies that

$$\Phi(x_b; E) - \Phi(x_a; E) = m\pi - \frac{\pi}{2} . \quad (A.14)$$

Finally then, we obtain

$$\theta'(E) = \frac{\partial}{\partial E}\arg\left(\frac{A(E)D(E)}{B(E)C(E)}\right) = 2\frac{\partial}{\partial E}\left[\int_{x_a(E)}^{x_b(E)} \sqrt{\frac{2m}{\hbar^2}}\sqrt{E - V(x)}\mathrm{d}x\right] = \int_{x_a(E)}^{x_b(E)} \sqrt{\frac{2m}{\hbar^2}}\frac{1}{\sqrt{E - V(x)}}\mathrm{d}x . \quad (A.15)$$

Note that the terms which contain the derivatives of $x_a(E)$ and $x_b(E)$ vanish due to these being classical turning points.

We wish to relate $\theta'(E_m)$ to the other parameters in the system and, in particular, to $|a_+(E_m)|^2$, which we determine by normalization of the energy eigenmodes. To do this, we need to choose the basis set of $u_E^{\pm}(x)$ modes. This set of modes is also needed to expand our initial conditions, so we require a set of u_E functions, defined on the entire x-axis, which are proportional to the WKB solutions in their region of validity $x_1 < x < x_2$, and further are delta-function normalizable:

$$\int_{-\infty}^{\infty}\left[u_{E_1}^{\pm}(x)\right]^*\left[u_{E_2}^{\pm}(x)\right] = \delta(E_1 - E_2) . \quad (A.16)$$

A convenient choice of the $u_E^{\pm}(x)$ is to make them solutions of a modified potential, which matches the real potential in the region $x_1 < x < x_2$. We choose the modified potential as

$$V_{\mathrm{NEW}}(x) = \begin{cases} V(x) & x_1 < x < x_2 \\ 0 & \text{otherwise} \end{cases} \quad (A.17)$$

which has the unnormalized energy eigenstates

$$\phi_{\mathrm{NEW}}^{\pm}(x, E) = \begin{cases} \frac{\mathrm{e}^{\mathrm{i}\Phi(x_b;E)}}{\sqrt[4]{\frac{2mE}{\hbar^2}}}\exp\left[\mathrm{i}(x - x_1)\sqrt{\frac{2mE}{\hbar^2}}\right] , & x < x_1 \\ \phi_{\mathrm{WKB}}^{\pm}(x, E) , & x_1 < x < x_2 \\ \frac{\mathrm{e}^{\mathrm{i}\Phi(x_a;E)}}{\sqrt[4]{\frac{2mE}{\hbar^2}}}\exp\left[\mathrm{i}(x - x_2)\sqrt{\frac{2mE}{\hbar^2}}\right] , & x > x_2 . \end{cases} \quad (A.18)$$

Noting that the complex exponential part dominates the normalization, and exploiting the well-known relation

$$\int_{-\infty}^{\infty}\exp[\mathrm{i}(k - k')x]\mathrm{d}x = 2\pi\delta(k - k') , \quad (A.19)$$

where, in this case $k = \sqrt{2mE/\hbar^2}$, we find

$$\int_{-\infty}^{\infty}\exp\left[\mathrm{i}\left(\sqrt{\tfrac{2mE}{\hbar^2}} - \sqrt{\tfrac{2mE'}{\hbar^2}}\right)x\right]\mathrm{d}x = 2\pi\delta(E - E')\sqrt{\frac{2\hbar^2 E}{m}} . \quad (A.20)$$

Using this relation gives the delta-function normalized energy eigenstates of the modified potential as

$$u_E^{\pm}(x) = \sqrt{\frac{m}{2\pi\hbar^2}}\phi_{\mathrm{NEW}}^{\pm}(x, E) . \quad (A.21)$$

To determine $|a_{+_m}|^2$, where $a_{\pm_m} = a_{\pm}(E_m)$ and E_m is an eigenenergy of the original potential, we need to normalize the mode functions, which, between x_1 and x_2, have the form

$$\phi_m(x) = a_{+_m}u_m^+(x) + a_{-_m}u_m^-(x) . \quad (A.22)$$

Our first approximation is that, due to the fact that we are using systems for which the WKB approximation is valid, the contribution is small outside the classical turning points, and as (x_1, x_2) can be brought sufficiently close to (x_a, x_b), we write

$$1 = \int_{-\infty}^{\infty}|\phi_m(x)|^2\mathrm{d}x \quad (A.23)$$

$$\approx \int_{x_a(E)}^{x_b(E)}|a_{+_m}u_m^+(x) + a_{-_m}u_m^-(x)|^2\mathrm{d}x . \quad (A.24)$$

As the $u_m^{\pm}(x)$ are highly oscillatory for the range of energies we are considering, the overlap $\int[u_m^{\pm}(x)]^2\mathrm{d}x$ is small, so we can write

$$1 \approx 2\int_{x_a(E)}^{x_b(E)}|a_{+_m}|^2|u_m^+(x)|^2\mathrm{d}x , \quad (A.25)$$

hence, we obtain $|a_{+_m}|^2$ as

$$|a_{+_m}|^2 = \frac{2\pi\sqrt{\frac{\hbar^2}{2m}}}{\int_{x_a(E)}^{x_b(E)}\frac{1}{\sqrt{E - V(x)}}\mathrm{d}x} \quad (A.26)$$

$$= \frac{2\pi}{\theta'(E_m)} . \quad (A.27)$$

So we have finally obtained the result

$$\sum_{i=0}^{\infty}\left(\frac{A(E)D(E)}{B(E)C(E)}\right)^{\mathrm{i}} = \sum_m |a_{+_m}|^2\delta(E - E_m) . \quad (A.28)$$

This may be a more general relation, and not depend upon the WKB approximations which have been used to obtain it, but the general result has not been proved.

Acknowledgements. This project was supported by the New Zealand Foundation for Research, Science and Technology and by the University of Auckland Research Committee.

References

1. O. Carnal, J. Mlynek: Phys. Rev. Lett. **66**, 2689 (1991)
2. D.W. Keith, C.R. Ekstrom, Q.A. Turchette, D.E. Pritchard: Phys. Rev. Lett. **66**, 2693 (1991)
3. M. Kasevich, S. Chu: Phys. Rev. Lett. **67**, 181 (1991)
4. F. Shimizu, K.Shimizu, H. Takuma: Phys. Rev. A **46**, 17 (1992)
5. V.I. Balykin, V.S. Letokhov: Appl. Phys. B **48**, 517 (1989)
6. H. Wallis, J. Dalibard, C. Cohen-Tannoudji: Appl. Phys. B **54**, 407 (1992)
7. M. Wilkens, E. Goldstein, B. Taylor, P. Meystre: Phys. Rev. A **47**, 2366 (1993)
8. M. Kasevich, D.S. Weiss, S. Chu: Opt. Lett. **15**, 607 (1990)
9. K. Helmerson, S.L. Rolston, L. Goldner, W.D. Phillips: In *Optics and Interferometry with Atoms*, Book of Abstracts, WE-Heraeus-Seminar, Konstanz (1992) (unpublished)
10. C.G. Aminoff, A.M. Steane, P. Bouyer, P. Desboilles, J. Dalibard, C. Cohen-Tannoudji: Phys. Rev. Lett. **71**, 3083 (1993)
11. W. Seifert, C.S. Adams, V.I. Balykin, C. Heine, Yu. Ovchinnikov, J. Mlynek: Phys. Rev. A (submitted)
12. A. Erdelyi (ed.): *Higher Transcendental Functions*, Vol. II (McGraw-Hill, New York 1953)